Stem Cell Reports
Article

ISSCR

OPEN ACCESS

Thyroid Hormone Transporters MCT8 and OATP1C1 Control Skeletal Muscle Regeneration

Steffen Mayerl,[1,2,3] Manuel Schmidt,[1] Denica Doycheva,[1,2] Veerle M. Darras,[4] Sören S. Hüttner,[1] Anita Boelen,[5] Theo J. Visser,[6] Christoph Kaether,[1] Heike Heuer,[2,7,*] and Julia von Maltzahn[1,*]

[1]Leibniz Institute on Aging/Fritz Lipmann Institute, Jena, Germany
[2]Leibniz Research Institute for Environmental Medicine, Düsseldorf, Germany
[3]MRC Centre for Regenerative Medicine, University of Edinburgh, Edinburgh, UK
[4]Laboratory of Comparative Endocrinology, Katholieke Universiteit Leuven, Leuven, Belgium
[5]Academic Medical Center (AMC), Amsterdam, The Netherlands
[6]Erasmus Medical Center (EMC), Rotterdam, The Netherlands
[7]University of Duisburg-Essen, University Hospital Essen, Department of Endocrinology, Essen, Germany
*Correspondence: heike.heuer@uk-essen.de (H.H.), julia.vonmaltzahn@leibniz-fli.de (J.v.M.)
https://doi.org/10.1016/j.stemcr.2018.03.021

SUMMARY

Thyroid hormone (TH) transporters are required for the transmembrane passage of TH in target cells. In humans, inactivating mutations in the TH transporter MCT8 cause the Allan-Herndon-Dudley syndrome, characterized by severe neuromuscular symptoms and an abnormal TH serum profile, which is fully replicated in *Mct8* knockout mice and *Mct8/Oatp1c1* double-knockout (M/O DKO) mice. Analysis of tissue TH content and expression of TH-regulated genes indicate a thyrotoxic state in *Mct8*-deficient skeletal muscles. Both TH transporters are upregulated in activated satellite cells (SCs). In *M/O* DKO mice, we observed a strongly reduced number of differentiated SCs, suggesting an impaired stem cell function. Moreover, *M/O* DKO mice and mice lacking both transporters exclusively in SCs showed impaired skeletal muscle regeneration. Our data provide solid evidence for a unique gate-keeper function of MCT8 and OATP1C1 in SC activation, underscoring the importance of a finely tuned TH signaling during myogenesis.

INTRODUCTION

Cellular entry and efflux of thyroid hormones (THs) are facilitated by transmembrane transporters such as the monocarboxylate transporters 8 (MCT8) and 10 (MCT10), organic anion transporting protein 1C1 (OATP1C1), and the L-type amino acid transporters LAT1 and LAT2 (Bernal et al., 2015; Heuer and Visser, 2009, 2013). MCT8, the most intensively studied TH transporter, is encoded by the *SLC16A2* gene and exhibits the highest specificity toward the prohormone 3,3′,5,5′-tetraiodothyronine (thyroxine; T4) and the active form 3,3′,5-triiodothyronine (T3) (Friesema et al., 2003, 2005; Visser et al., 2011). Inactivating mutations in MCT8 were identified to underlie the clinical picture of the Allan-Herndon-Dudley syndrome (AHDS), a severe form of psychomotor retardation (Dumitrescu et al., 2004; Friesema et al., 2004; Schwartz et al., 2005). As a hallmark of this disease, patients present characteristic alterations in the serum TH profile with highly elevated T3 and decreased T4 concentrations along with signs of a peripheral thyrotoxicity such as hypermetabolism, low body weight, and muscle wasting. Moreover, affected patients suffer from pronounced neuromuscular abnormalities and uncontrolled motor movements (Dumitrescu et al., 2004; Schwartz et al., 2005).

In order to gain insights into the pathogenic mechanisms of AHDS, *Mct8* knockout (KO) mice were generated (Dumitrescu et al., 2006; Trajkovic et al., 2007; Wirth et al., 2009). Though these *Mct8* KO mice fully replicate the abnormal serum TH profile and the peripheral hyperthyroidism of AHDS patients, they do not show any neurological impairment or behavioral abnormalities (Ceballos et al., 2009; Trajkovic et al., 2007). Indeed, we recently demonstrated that, in mice, only the concomitant inactivation of two TH transporters, MCT8 and OATP1C1 (encoded by the *Slco1c1* gene), results in a strongly diminished transport of TH across the blood-brain barrier (BBB) and, consequently, in highly reduced TH concentrations within the CNS (Mayerl et al., 2014). Since, in rodents, OATP1C1 is strongly expressed in brain endothelial cells but absent in endothelial cells of the primate CNS (Ito et al., 2011; Roberts et al., 2008), it has been postulated that OATP1C1 can compensate for the loss of MCT8 at the BBB in mice but not in humans.

Despite their central state of TH deprivation, *Mct8/Oatp1c1* double-knockout (M/O DKO) mice show a similar state of peripheral hyperthyroidism as *Mct8* KO mice. Moreover, unlike the single-mutant animals, only *M/O* DKO mice exhibit pronounced behavioral alterations including an ataxic gait and reduced locomotor performance making it a suitable model for AHDS (Mayerl et al., 2014).

Skeletal muscle is a major target of TH signaling, and changes in TH homeostasis are often linked to myopathic symptoms (Lee et al., 2014; Salvatore et al., 2014). Among those factors that are transcriptionally regulated by TH are

contractility determining proteins such as myosin heavy chain (MHC) type I (MHCI), MHCIIa, MHCIIb, and MHCIIx, and the transcription factors MYOD and MYOGENIN, which are essential for myogenesis and regeneration. The latter represents a highly orchestrated process that is triggered upon muscle injury and involves the activation of quiescent muscle stem cells (satellite cells [SCs]) followed by proliferation of myoblasts, their differentiation into myocytes, terminal fusion into myotubes, and the final maturation of newly formed myofibers (Bentzinger et al., 2012).

Here, we elucidate SC function and regenerative capacity in *Mct8/Oatp1c1*-deficient mice. We demonstrate that both TH transporters become upregulated in activated SCs and that a combined *Mct8/Oatp1c1* deficiency results in impairments in SC differentiation, thereby leading to a delayed skeletal muscle regeneration. Therefore, our study is the first that demonstrates a gate-keeper function of TH transporters within the precisely coordinated progression of SC activation and the differentiation program.

RESULTS

Thyroidal State of Skeletal Muscles

Mct8 deficiency in male mice leads to highly elevated serum T3 concentrations and rather low serum T4 levels while inactivation of *Oatp1c1* in male mice does not affect serum TH concentrations (Dumitrescu et al., 2006; Mayerl et al., 2012; Trajkovic et al., 2007). In order to rule out any sex-specific differences in TH status, we now also determined serum TH concentrations in 4-month-old female TH transporter mutants and found similar TH values indicating that *Mct8* deficiency in females fully replicates the TH abnormalities described in males (Figure 1A). Determination of tissue TH content in tibialis anterior (TA) muscle preparations from these mice revealed normal T3 and T4 values in *Oatp1c1* KO mice (Figure 1B), whereas the T3 content was found to be 3.5-fold elevated in *Mct8* KO and *M/O* DKO animals. Interestingly, *Mct8* KO mice showed normal tissue T4 values in TA muscle preparations, whereas the muscle T4 concentrations of *M/O* DKO mice were significantly decreased.

Local tissue TH concentrations are strongly influenced by the activities of TH metabolizing iodothyronine deiodinases type 2 (D2) and type 3 (D3), which can activate and inactivate TH by outer-ring and inner-ring deiodination, respectively (Bianco et al., 2002). Compared with control animals, *Mct8* KO mice exhibited a 3-fold increase in muscle D2 activities, while D3 values were not altered (Figure 1C). Remarkably, *M/O* DKO animals showed even a 6-fold rise in D2 activities, which might explain the drop in muscle T4 content in these animals. Concomitantly, D3 activities were significantly elevated in *M/O* DKO mice compared with respective levels in wild-type (WT) and *Mct8* KO animals, and a trend toward higher D3 activities was also observed in *Oatp1c1* KO mice. These findings point to distinct changes in skeletal muscle TH homeostasis in the absence of MCT8 and OATP1C1.

To investigate the functional consequences of this perturbed TH homeostasis in skeletal muscle we performed real-time qPCR (qPCR) analysis of TA muscle samples (Figure 1D). *D2* mRNA levels were largely in line with the enzymatic activities, whereas *D3* transcript levels were close to the detection limit and therefore did not reveal any significant alterations. Expression of *Hairless*, a gene positively regulated by TH, was strongly increased in *Mct8* KO and *M/O* DKO mice (Di Cosmo et al., 2013), while mRNA expression of *MhcI*, which is negatively regulated by TH (Soukup and Smerdu, 2015), was suppressed in *Mct8*-deficient mice. Likewise, transcript levels of *MhcIIa*, *MhcIIb*, and *MhcIIx*, known to be stimulated by TH (Soukup and Smerdu, 2015), tended to be elevated in *Mct8* KO and *M/O* DKO mice. Together, these results are indicative of a hyperthyroid state of skeletal muscle in the absence of MCT8, and MCT8 and OATP1C1. Importantly, *MyoD1* mRNA levels, a marker for activated SCs, did not show a rise in muscle tissue of *Mct8* KO and *M/O* DKO mice, suggesting that the changes in TH homeostasis did not lead to activation of SCs, which would be indicative of a phenotype resembling muscular dystrophy (Chang et al., 2016).

Next, we investigated muscle fiber type composition using antibodies recognizing either MHCI (slow MHC) only or all fast MHC isoforms (MHCIIa, IIb, and IIx). We found a reduction in the percentage of muscle fibers expressing slow MHC as well as an increase in the percentage of muscle fibers expressing fast MHC isoforms in *Mct8* KO and *M/O* DKO mice. Importantly, we found this shift in fiber types both in the soleus muscle (Figure 2A) and in the plantaris muscle (Figure 2B), the former consisting of primarily slow fibers, while the latter comprises mostly faster muscle fibers. These findings prompted us to subsequently clarify the cellular distribution of MCT8 and OATP1C1 in muscle tissue.

MCT8 and OATP1C1 Show Distinct Expression Patterns during Myogenesis

To obtain a broad overview of the expression pattern of different TH hormone transporters (Bernal et al., 2015) during myogenesis, we took advantage of our previously published Affymetrix microarray gene expression analysis (Price et al., 2014). Thereby, we compared freshly isolated (quiescent) SCs, SC-derived myoblasts, and differentiating myotubes (Figure 3A). Interestingly, *Mct8* as well as *Mct10* showed highest signal intensities in quiescent SCs. High transcript levels were also found for the L-type amino

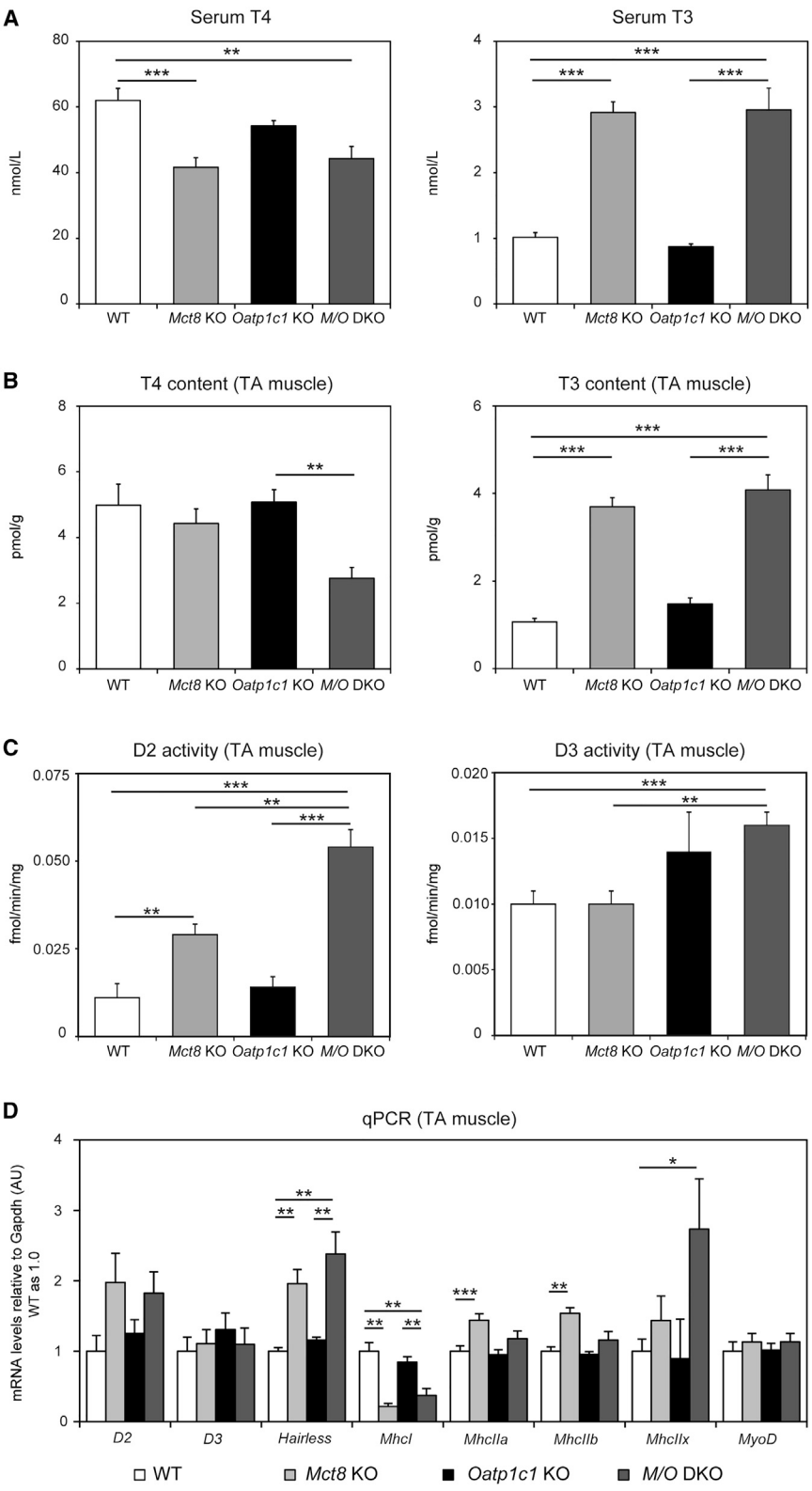

Figure 1. Thyroid State of Skeletal Muscle in TH Transporter-Deficient Mice

(A) Measuring serum TH concentrations in 4-month-old female mice (n = 8) revealed highly elevated serum T3 and decreased serum T4 values in *Mct8* deficiency, thereby replicating the characteristic TH serum profile of male *Mct8* KO animals.

(B) TA muscle T3 content was almost 4-fold elevated in *Mct8* KO and *M/O* DKO mice, while muscle T4 levels were reduced in *M/O* DKO mice only (n = 4 *Mct8* KO; n = 5 WT, *Oatp1c1* KO, *M/O* DKO mice).

(C) D2 and D3 enzymatic activities were measured in TA muscle homogenates. *M/O* DKO mice showed a pronounced rise in D2 and D3 activities (n = 6).

(D) qPCR analyses were performed using TA muscle homogenates from 2- to 3-month-old female mice to assess transcript levels of TH-regulated genes.

Group means + SEM are shown. n = 3 *Mct8* KO; *M/O* DKO; n = 5 WT, *Oatp1c1* KO mice. *p < 0.05; **p < 0.01; ***p < 0.001. Two-way ANOVA and Bonferroni-Holm post hoc testing.

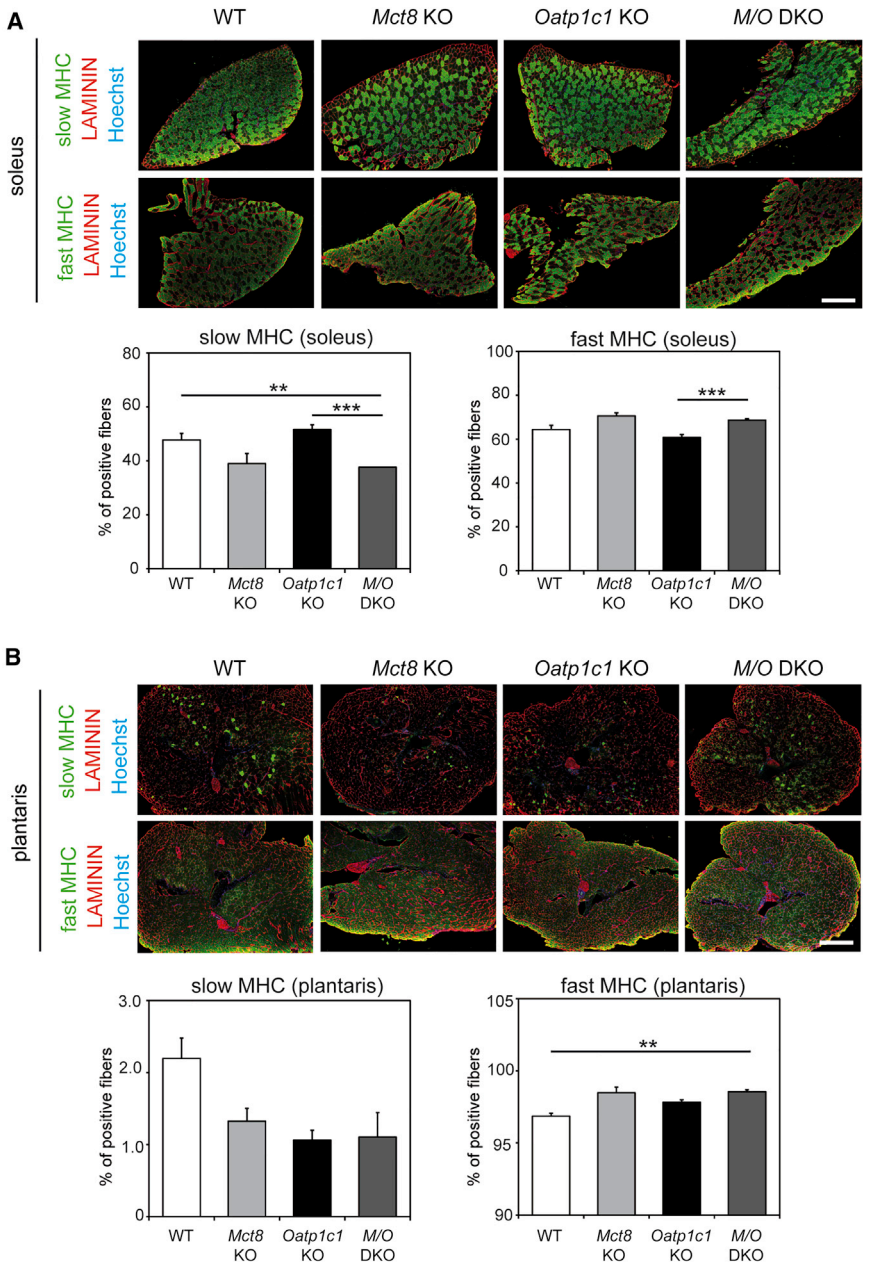

Figure 2. Analysis of Muscle Fiber Type Composition in TH Transporter-Deficient Mice

(A) Soleus cryosections were immunostained to visualize slow MHC or all fast MHC isoforms (in green) and co-labeled with an anti-LAMININ antibody (in red) to visualize myofiber boundaries; nuclei stained in blue. Quantification revealed a reduced percentage of slow MHC-positive fibers and a concomitant increase in the percentage of fast MHC-positive fibers in the absence of MCT8, and MCT8 and OATP1C1.

(B) Plantaris cryosections were immunostained to visualize slow MHC or all fast MHC isoforms (in green) and co-labeled with an anti-LAMININ antibody (in red); nuclei stained in blue. Similar trends could be observed.

Group means + SEM are shown. n = 3 *Mct8* KO, *Oatp1c1ko*; n = 6 WT, *M/O* DKO mice. **p < 0.01; ***p < 0.001. Two-way ANOVA and Bonferroni-Holm post hoc testing. Scale bar: 500 μm.

acid transporter *Lat1* (*Slc7a5*), which appears to be present in all myogenic cell types, while *Lat2* (*Slc7a8*) and *Oatp1c1* mRNA expression were rather low in all cell types analyzed.

Unfortunately, our array analysis did not provide any information about the expression profile of genes present in activated SCs. We therefore isolated primary extensor digitorum longus (EDL) myofibers with their adjacent SCs from 4-month-old female WT mice and analyzed expression of MCT8 and OATP1C1 in quiescent (0 hr), activated (42 hr), and differentiated (72 hr) SCs by immunocytochemistry (Figure 3B). The specificities of the immunofluorescence signals were confirmed by concomitant processing and staining of EDL myofibers from *M/O* DKO mice that were devoid of any specific labeling (data not shown). Immediately after the isolation of WT fibers, faint MCT8 staining was observed in PAX7-positive, still quiescent SCs, whereas OATP1C1-specific staining was not detectable (Figure 3B). Intriguingly, with increasing time in culture leading to activation, proliferation, and differentiation of SCs, expression of both TH transporters became visible in PAX7-positive cells, indicating that MCT8 and OATP1C1 expression is strongly upregulated in activated SCs.

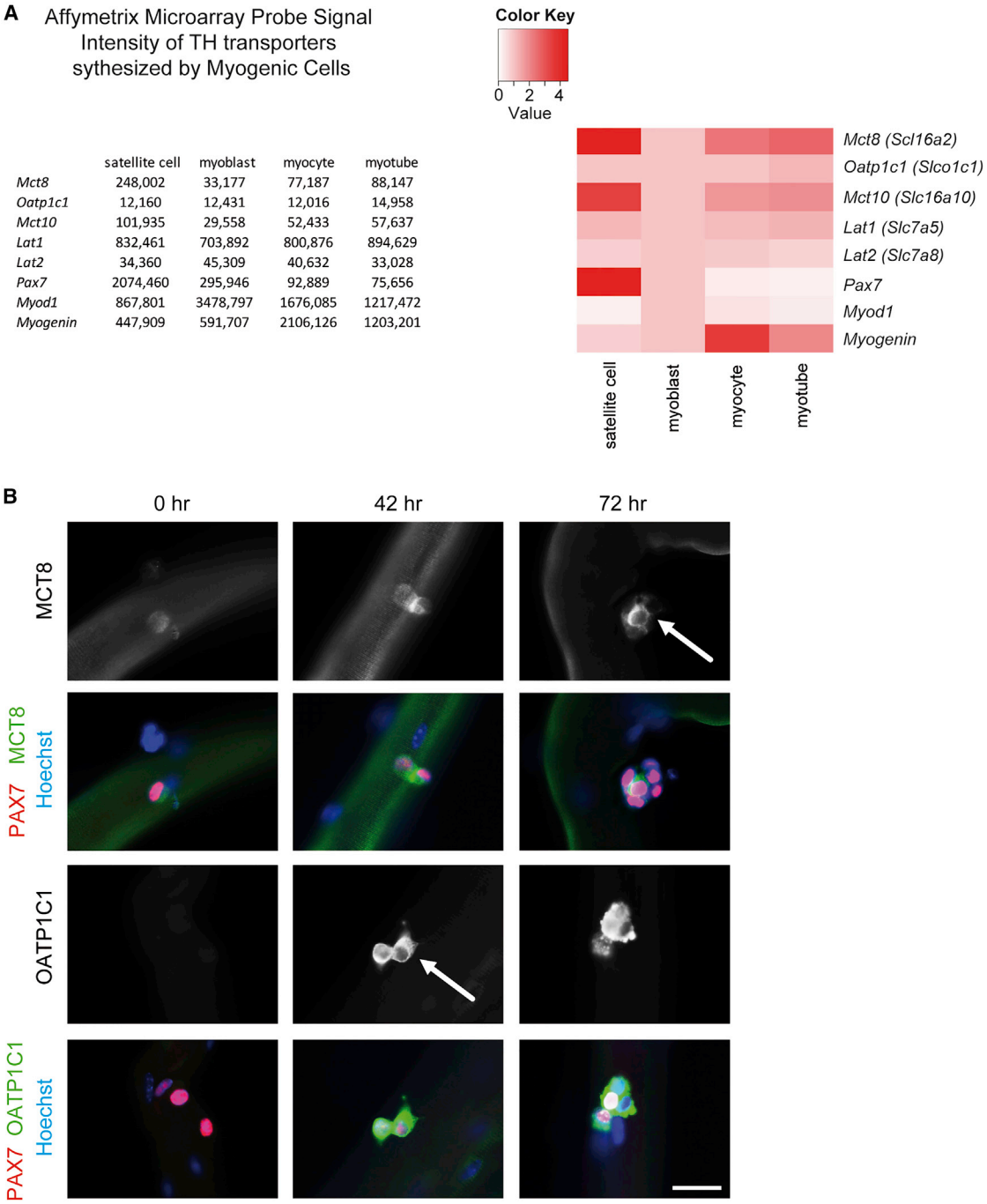

Figure 3. TH Transporter Expression in SCs

(A) Fold changes based on log_2-transformed RNA values from quiescent SCs, cultured myoblasts, myocytes, and myotubes were used to generate global ratio heat maps. While *Lat1* is highly expressed in all cell types, *Mct8* and *Mct10* exhibit strongest expression in SCs. *Oatp1c1* and *Lat2* mRNA levels are low compared with *Mct8*.

(B) Primary EDL myofibers isolated from female WT mice and cultured for 0, 42, or 72 hr.

Immunofluorescence studies revealed MCT8 expression (in green, arrow) in PAX7-positive (red) SCs at all analyzed time points. In comparison, OATP1C1 (in green, arrow) could not be detected at 0 hr but was clearly visible after 42 and 72 hr in PAX7-positive (in red) SCs. Nuclei stained in blue. Representative images of n = 3. Scale bar: 5 μm.

THs are known to orchestrate the differentiation process within the myogenic program (Dentice et al., 2013). Therefore, we wondered whether the absence of MCT8 and/or OATP1C1 might interfere with the activation and differentiation of SCs. Hence, EDL myofibers were isolated from WT and TH transporter-deficient, 4-month-old female mice and analyzed directly or after 72 hr in culture. Staining for the SC marker PAX7 and the differentiation marker MYOD demonstrated no aberrant activation of SCs under resting conditions in TH transporter-deficient mice (Figure 4A). Though the overall percentage of PAX7-positive cells per cluster was comparable between the genotypes after 72 hr in culture (Figure S1A), differences in their differentiation state became apparent: the percentage of non-differentiated SCs expressing only PAX7, but not MYOD, per cluster was almost doubled in EDL cultures of *Mct8/Oatp1c1* DKO mice (Figure 4B), whereas the percentage of committed SCs (PAX7/MYOD double-positive) was reduced by 47% (Figure 4C), suggesting a delay in differentiation of SCs. In addition, the overall percentage of MYOD-expressing cells per cluster was significantly decreased in MCT8 and OATP1C1 deficiency (Figure 4D), but not the percentage of only MYOD-positive myoblasts (Figure S1B). Obviously, a combined MCT8 and OATP1C1 inactivation compromises directly and/or indirectly SC differentiation *in vitro*.

As an additional *in vitro* approach to clarify the muscle-specific function of MCT8 and OATP1C1 and to avoid possible compensatory effects, we prepared EDL fiber cultures from WT and *Oatp1c1* KO mice that show normal serum TH values and a normal muscle TH content. These fiber cultures were treated for 72 hr with Silychristin (25 μM) as this compound has been recently shown to specifically inhibit Mct8 (Johannes et al., 2016). Immunostaining of fiber cultures with PAX7 and MYOD indeed revealed the highest number of cells expressing only PAX7 in *Oatp1c1* KO mice treated with Silychristin (Figure 4E), whereas the percentage of PAX7-positive cells per cluster was not altered (Figure S1C). Likewise, the percentage of PAX7/MYOD-positive, differentiated SCs was slightly reduced in Silychristin-treated cultures (Figure 4F), though neither the percentage of MYOD-expressing cells nor the percentage of MYOD only-positive nuclei were significantly affected by the inhibitor treatment (Figures 4G and S1D). Altogether, these *in vitro* data suggest an impaired differentiation of SCs entering the myogenic program in the absence of MCT8 and OATP1C1.

Muscle Regeneration and SC Differentiation Are Impaired *In Vivo* in TH Transporter-Deficient Mice

We wondered whether impairments in the myogenic program also occur *in vivo* after injury when both TH transporters are absent. Therefore, we injured the TA muscle of adult female mice by injection of cardiotoxin (CTX).

First, we investigated myofiber size in resting conditions but did not observe significant differences between the genotypes by analyzing the minimal fiber feret (diameter) as a measure of fiber size (Figures 5A and 5B). Intriguingly, 5 days after CTX injection (5 days post injury [dpi]), the minimal fiber feret was reduced in all TH transporter-deficient animals, with the most pronounced and statistically significant reduction in *M/O* DKO mice (14.4 μm compared with 20.5 μm in WT animals). This impaired regeneration was still evident at 10 dpi when fiber size was still clearly reduced in all TH transporter KO mice, with lowest values in *M/O* DKO animals (19.7 μm compared with 25.2 μm in WT controls). Interestingly, we did not observe significant differences in myofiber size at 21 dpi, suggesting rather a delay in regeneration than a general inhibition in the absence of MCT8 and OATP1C1.

Since regeneration of skeletal muscle depends on functional SCs (Lepper et al., 2011; Murphy et al., 2011; von Maltzahn et al., 2013), we speculated that the delayed regeneration of *M/O* DKO mice is due to impaired SC function. Therefore, we enumerated the number of SCs expressing PAX7 and SCs that also express the differentiation marker MYOD at different time points after injury as well as under resting conditions (Figure 6A). Surprisingly, already under resting conditions we found a 2.1-fold increase in the number of PAX7-positive SCs in *M/O* DKO mice, suggesting alterations in apoptosis and/or proliferation of SCs in the absence of both TH transporters (Figure 6B). Quantification of proliferating KI67-positive cells, however, revealed similar numbers under basal conditions in all TA sections, arguing against pronounced alterations in SC proliferation in *Mct8/Oatp1c1* deficiency (Figure 6C). Likewise, counting of PAX7/TUNEL double-positive cells did not show any significant differences between the genotypes as the number of apoptotic PAX7 cells were, as expected, in general very low under basal conditions (Figure 6D). Thus, we exclude differences in proliferation or apoptosis as the cause for the elevated numbers of SCs in MCT8- and OATP1C1-deficient muscles.

Quantification of PAX7-positive cells at 5 dpi demonstrated decreased numbers in *Mct8*-deficient muscles, while *Oatp1c1* and *M/O* DKO muscles did not show significant differences compared with control mice (Figure 6E), in the latter case possibly due to the higher number of SCs under resting conditions. Importantly, we observed significantly reduced numbers of PAX7/MYOD-positive SCs 5 dpi in *Mct8* KO and *M/O* DKO muscles, suggesting impairments in either activation or differentiation. This prompted us to quantify PAX7- and MYOD-positive cells at later time points (10 dpi and 21 dpi). Notably, we found reduced numbers of PAX7/MYOD double-positive cells at 10 dpi in

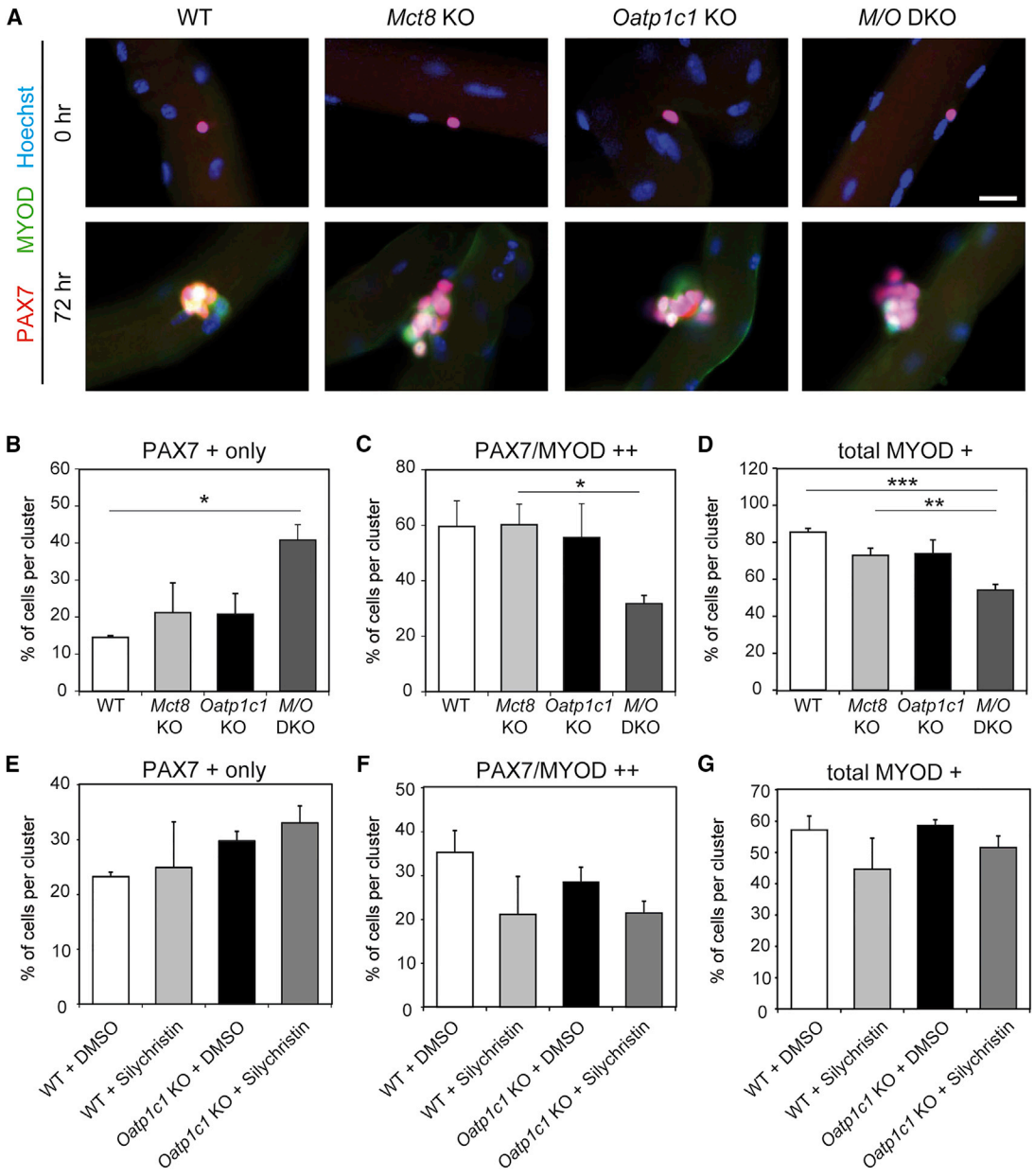

Figure 4. SC Activation and Differentiation Is Delayed in Myofiber Cultures of *M/O* DKO Mice

(A) WT, *Mct8*-, and/or *Oatp1c1*-deficient primary EDL myofibers (n = 3) were either fixed directly (0 hr) or cultured for 72 hr and incubated with antibodies against PAX7 (in red) and the activation and differentiation marker MYOD (green) as well as with Hoechst33528 to label cell nuclei (in blue). MYOD immunoreactivity was only detected after 72 hr of culture as expected.

(B) Marker-positive cell nuclei were quantified and revealed a higher percentage of PAX7 only immunopositive nuclei in *M/O* deficiency at 72 hr.

(C–D) Both the percentage of PAX7/MYOD double-positive (C) and total MYOD-positive (D) nuclei per cluster were reduced in cultures derived from *M/O* DKO mice.

(E–G) EDL myofibers from WT (n = 4) and *Oatp1c1* KO mice (n = 6) were cultured for 72 hr with the MCT8 inhibitor Silychristin or DMSO. Analysis of PAX7- and MYOD-immunopositive cells demonstrated a tendency toward a higher number of PAX7+ only cells (E) and a reduced number of PAX7/MYOD-immunopositive cells (F), but not toward total MYOD-positive cell numbers (G) in Silychristin-treated *Oatp1c1*-deficient myofibers. These findings support a delayed SC activation and differentiation if OATP1C1 and MCT8 are absent or inhibited. Group means + SEM are shown.

*p < 0.05; **p < 0.01; ***p < 0.001. Two-way ANOVA and Bonferroni-Holm post hoc testing. Scale bar: 10 μm.

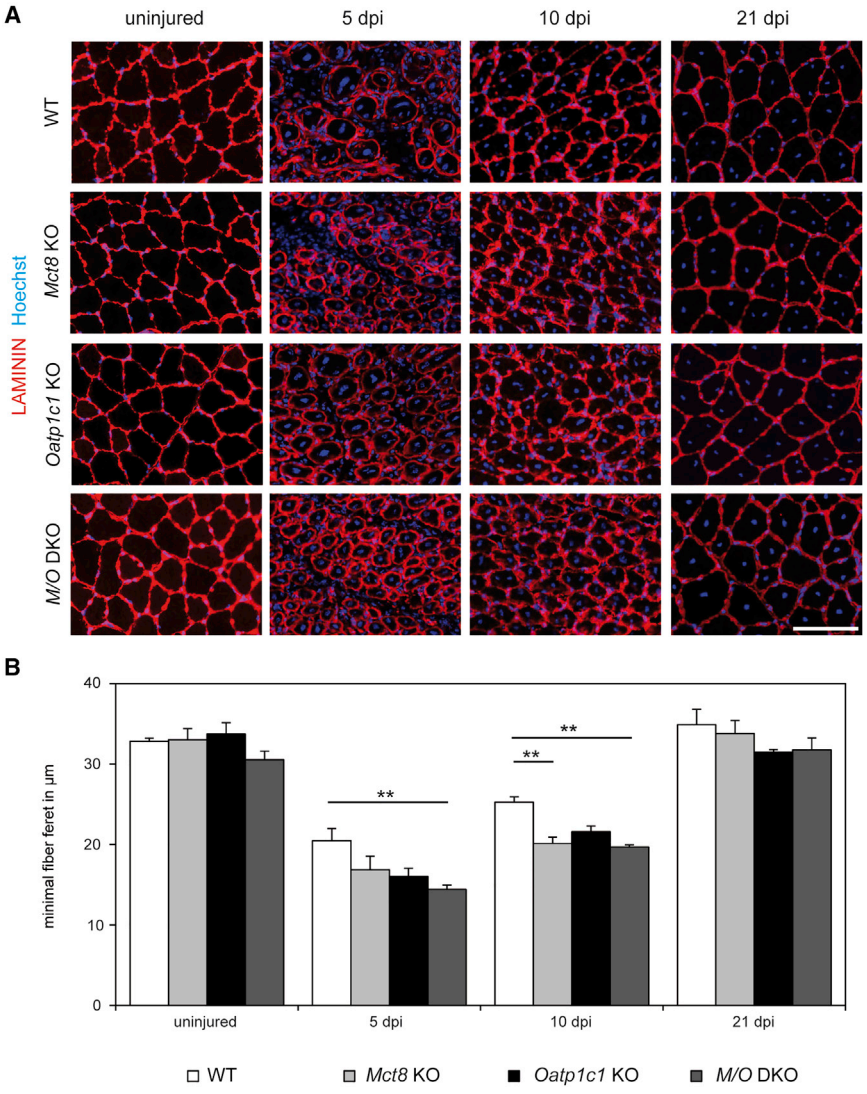

Figure 5. Compromised Muscle Regeneration in *M/O* DKO Mice

(A) The TA muscle of female mice was injured with CTX at the age of 2.5–4 months and mice were sacrificed 5, 10, or 21 dpi. TA cryosections were incubated with an anti-LAMININ antibody (in red) to visualize myofiber boundaries and Hoechst 33258 (in blue).

(B) No differences in myofiber size were found in TH transporter mutant animals under basal condition. Upon injury (5 and 10 dpi), *Oatp1c1* KO, *Mct8* KO, and *M/O* DKO mice presented reduced myofiber diameters with smallest fibers in *M/O* DKO animals. At 21 dpi, minimal fiber feret was similar in all animal groups, indicating that, in the absence of *Mct8* and/or *Oatp1c1*, muscle fiber regeneration is only temporarily delayed.

Group means + SEM are shown. n = 4 WT 5 dpi, *M/O* DKO 5 dpi; n = 3 all other groups. **p < 0.01. Two-way ANOVA and Bonferroni-Holm post hoc testing. Scale bar: 50 µm.

M/O DKO mice, while numbers of PAX7-positive cells were not significantly altered at 10 dpi or 21 dpi (Figures 6E and 6F), suggesting inhibition of the differentiation process.

One may speculate that the abnormal serum profile and, consequently, the global changes in muscle TH content contribute to the delayed regenerative capacity in *Mct8*-deficient animals. To exclude any systemic effects due to the global loss of *Mct8* and/or *Oatp1c1*, we generated mice with a specific inducible deletion of both TH transporters in SCs (Figure S2A).

For that purpose, we obtained conditional *Mct8* mouse mutants from the KOMP (Knockout Mouse Project) repository that carry *loxP* sites flanking exon 3 of the murine *Mct8* gene (Figure S2A). Cre recombinase-mediated deletion of exon 3 was predicted to result in a frameshift mutation from exon 4 to 5 and thus loss of function of the *Mct8* gene product. *Mct8* fl/fl or *Mct8* fl/y mice were mated with *Oatp1c1* fl/f (Mayerl et al., 2012) mice and mice carrying the *Pax7 CreERT2* transgene (Murphy et al., 2011). CRE recombinase activity was induced prior to all experiments by tamoxifen. The successful removal of both *Mct8* exon 3 and *Oatp1c1* exon 3 was confirmed on DNA level (Figure S2B). To further prove that our cell-specific KO strategy was successful, we isolated EDL muscle fibers from *M/O*-SC KO animals and analyzed MCT8 and OATP1C1 expression by immunostaining after 72 hr of culture. TH transporter-specific fluorescent signals were absent in 70% of PAX7-positive cell clusters (Figures 7A, 7B, and S2C), suggesting that Cre recombinase-mediated inactivation of *Mct8* and *Oatp1c1* was not complete but was efficient enough for further analysis. As expected, *M/O*-SC KO mice were phenotypically indistinguishable from control animals and exhibited normal serum TH parameters (Figure S2D).

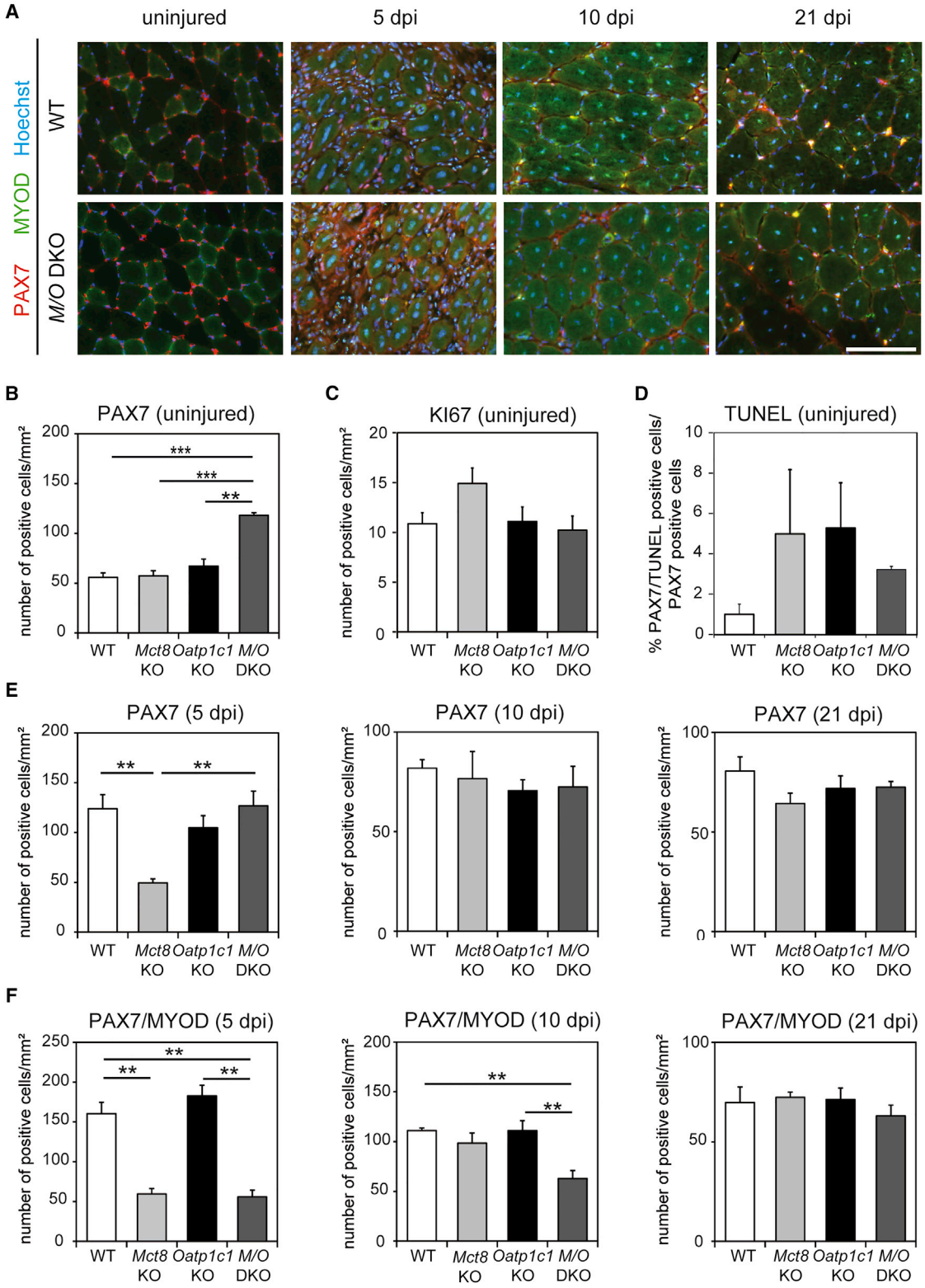

Figure 6. Delayed SC Activation and Differentiation in *M/O* DKO Mice upon Injury

(A) The TA muscle of female mice was injured with CTX at the age of 2.5–4 months and mice were sacrificed 5, 10, or 21 dpi. TA sections were stained for the SC marker PAX7 (in red), the early differentiation factor MYOD (in green), and Hoechst 33258 (in blue). Representative images for WT and *M/O* DKO mice are depicted.

(legend continued on next page)

We injured the TA muscle of young adult female *M/O*-SC KO mice and analyzed muscle regeneration at 10 dpi. Importantly, we did not observe differences in SC numbers under resting conditions between *M/O*-SC KO and control mice (Figure S2E). After injury, we found a significant decrease in the number of PAX7/MYOD double-positive SCs (Figures 7C and 7D) and myofiber size (Figures 7E and 7F) resembling the phenotype of *M/O* DKO mice. This prompted us to conclude that MCT8 and OATP1C1 fulfill SC-specific functions during regeneration.

DISCUSSION

Skeletal muscle is a well-established TH target tissue as TH regulates the expression of numerous muscle proteins critical for proper muscle development and contractility (Ambrosio et al., 2017; Milanesi et al., 2016, 2017; Soukup and Smerdu, 2015). Thus, highly elevated serum T3 levels, as detected in AHDS patients, are expected to heavily affect skeletal muscle homeostasis and regeneration. Elevated T3 levels may even cause or contribute to the overt muscle wasting and locomotor deficits of these patients. Indeed, increased serum concentrations of lactic acid and ammonemia as markers of skeletal muscle catabolism are indicative for a thyrotoxic state of skeletal muscle tissues in those patients (Herzovich et al., 2007). Likewise, *Mct8* KO mice as well as *M/O* DKO mice, which both replicate the abnormal circulating TH concentrations of the patients (Dumitrescu et al., 2006; Mayerl et al., 2014; Trajkovic et al., 2007) (Figure 1A), show an almost 4-fold increase in TA muscle T3 content (Figure 1B). This rise in T3 is accompanied by an increased expression of the T3-regulated target gene *hairless*. Furthermore, expression analysis of different MHC isoforms and analysis of the fiber type distribution in different skeletal muscles (Figures 1D and 2) indicate a shift from slow-twitch to fast-twitch fibers as expected from a hyperthyroid muscle tissue (Figure 2) (Soukup and Smerdu, 2015). These observations are in line with previous data describing increased skeletal muscle T3 content and TH action in *Mct8* KO mice (Di Cosmo et al., 2013).

One might even suggest that MCT8 does not play a major role in muscle TH transport as the circulating T3 levels appear to be fully sensed by MCT8-deficient skeletal muscle cells. Of note, *Mct10*, a close relative of *Mct8* and a potent T3 transporter (Friesema et al., 2008), shows a similar skeletal muscle expression pattern as *Mct8* according to our cell-specific RNA profiling (Figure 3A). Thus, as also suggested by Di Cosmo et al. (2013), MCT10 might at least partially compensate for the absence of MCT8 in the murine muscle. Such a scenario could be tested by assessing the thyroidal skeletal muscle phenotype of *Mct10/Mct8* DKO mice, particularly as studies of double-mutant animals have already shown a concerted action of MCT10 and MCT8 in mediating TH transport in liver, kidneys, and the thyroid (Müller et al., 2014). However, it also should be kept in mind that muscle tissue contains various cell types with distinct TH transporter repertoire. Thus, the cell-specific TH status may vary greatly between different skeletal muscle cell types in mice that lack *Mct8* globally.

That this is indeed the case becomes already evident with the determination of T4 concentrations and deiodinase activities in skeletal muscle homogenates. Despite the low T4 levels in the circulation, skeletal muscle T4 content was found to be surprisingly normal in *Mct8* KO mice. The observed increased mRNA levels and activities of the TH-activating enzyme *D2* would be indicative of a hypothyroid state, although the total tissue T3 content and our qPCR data argue for a thyrotoxic situation in TA muscle (Figures 1B–1D). A different situation was found in *M/O* DKO mice that displayed reduced T4 muscle content in combination with highly elevated D2 and increased activities of the TH-inactivating enzyme D3 (Figure 1C). A simultaneous rise in D2 and D3 activities is contradictory to general expectations as D2 is negatively and D3 is positively regulated by TH (Bianco et al., 2002). Rather, our observations point to muscle-intrinsic, cell-specific changes in TH homeostasis in *Mct8* KO or *M/O* DKO muscles, with some cells being in a hyperthyroid and others in a hypothyroid state. As another explanation, *M/O* DKO mice present a more than 2-fold increase in the number of SCs at baseline, which are the main cellular source of *D3* expression in skeletal muscle (Dentice et al., 2014). Hence, the high D3 activities in those animals might simply reflect the increased number of *D3*-expressing cells *in vivo*.

(B) Quantification of marker analyses in the uninjured state revealed a significantly increased number of PAX7-positive cells in *M/O* DKO animals.
(C–D) However, this increase is neither due to increased proliferation nor decreased apoptosis of SCs as both KI67 staining (C) and TUNEL staining of PAX7-positive nuclei (D) did not reveal any significant changes between the genotypes.
(E) Upon injury the number of PAX7-positive SCs was decreased in *Mct8* KO mice at 5 dpi, while at 10 and 21 dpi the different groups showed similar numbers.
(F) Enumeration of PAX7/MYOD double-positive cells revealed reduced numbers in *Mct8* KO and *M/O* DKO animals at 5 dpi. At 10 dpi, a significant drop in PAX7/MYOD-positive cells was only found in *M/O* DKO mice.
Group means + SEM are shown. n = 4 WT 5 dpi, *M/O* DKO 5 dpi; n = 3 all other groups.
**p < 0.01; ***p < 0.001. Two-way ANOVA and Bonferroni-Holm post hoc testing. Scale bar: 50 μm.

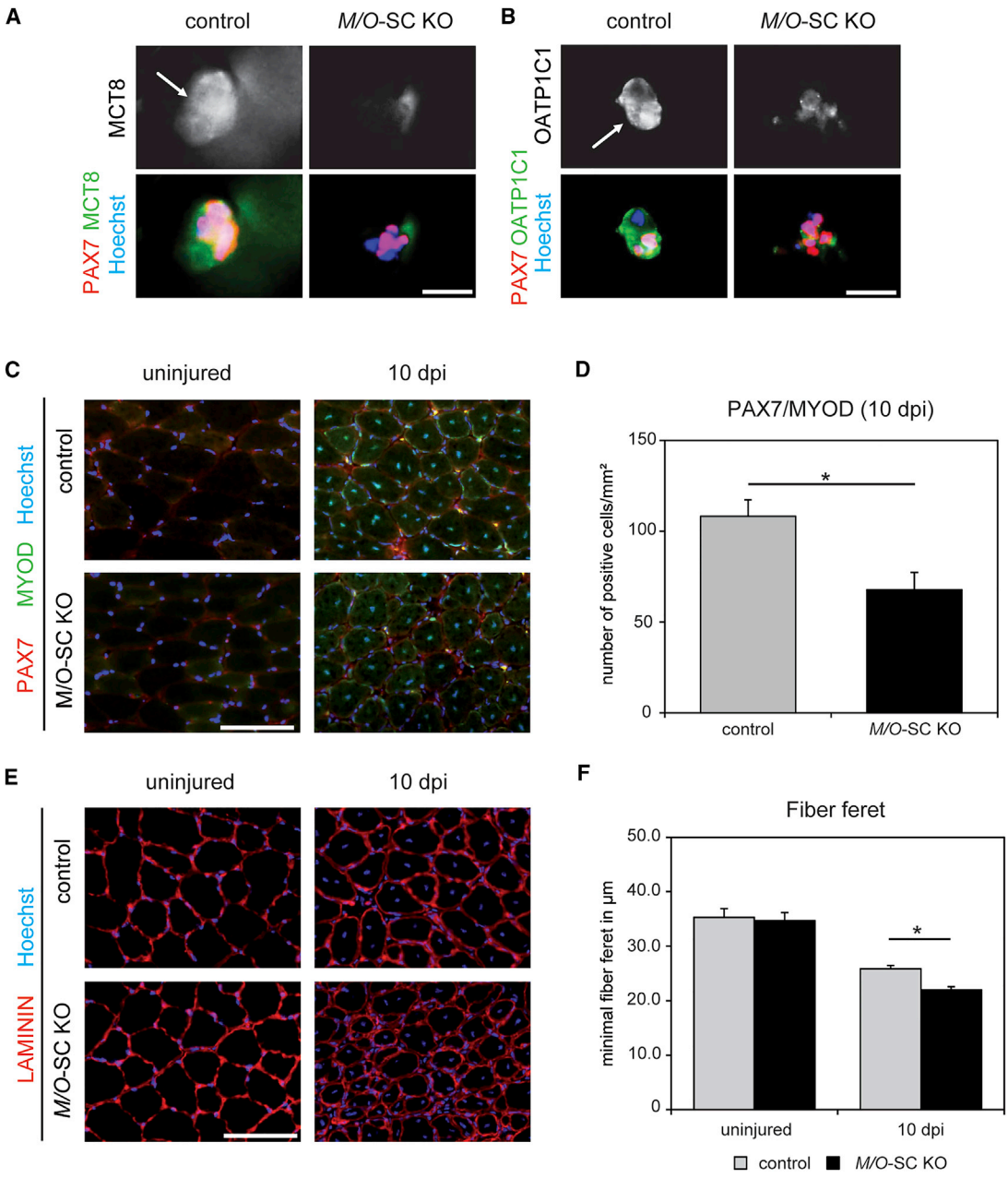

Figure 7. Compromised Muscle Regeneration upon Conditional Inactivation of *Mct8* and *Oatp1c1* in SCs. EDL Myofibers Were Isolated from Tamoxifen-Treated Control and *M/O*-SC KO Littermates and Cultured for 72 hr

(A and B) Immunofluorescence staining for MCT8 (in green) (A) and OATP1C1 (in green) (B) demonstrated signals in clusters of PAX7-positive cells (red) in control samples, whereas signal intensities were strongly reduced in *M/O*-SC KO animals (nuclei in blue). Arrows depict cells positive for PAX7 and MCT8 or PAX7 and OATP1C1, respectively.

(C) TA muscles of 3-month-old control and *M/O*-SC KO mice were injured with CTX and analyzed by immunostainings 10 dpi (PAX7 in red; MYOD in green, nuclei in blue).

(D) Quantification showed a significantly reduced number of PAX7/MYOD double-positive SCs in *M/O*-SC KO mice.

(E) Immunofluorescence staining for LAMININ (in red) and cell nuclei (in blue) indicated similar fiber diameters in TA muscles in the uninjured state, while *M/O*-SC KO animals showed a reduced myofiber size at 10 dpi.

(F) Minimal fiber feret determination in uninjured TA muscle revealed similar numbers. However, injured TA muscles of *M/O*-SC KO mice revealed a reduced myofiber diameter 10 dpi. Group means + SEM are shown. n = 4.

*$p < 0.05$, unpaired 2-tailed Student's t test. Scale bars: 5 µm (A and B) and 50 µm (C and E).

In a first approach to unravel the muscle-specific functions of MCT8 and OATP1C1 we determined the cell-type-specific expression patterns of these two transporters. It has already been reported that *Mct8* transcripts are present in skeletal muscle tissue (Di Cosmo et al., 2013), and our cell-type-specific profiling as well as immunohistochemical data are in line with this earlier report. Intriguingly, we could detect strongest MCT8 expression in quiescent and activated SCs, whereas OATP1C1 protein expression was only transiently observed in activated SCs (Figure 3). This temporally regulated expression pattern indeed suggested a specific function of both transporters in SCs that are required for regeneration of skeletal muscle (Lepper et al., 2011; Murphy et al., 2011; von Maltzahn et al., 2013).

TH tightly regulates muscle regeneration as unambiguously demonstrated in various studies (Dentice et al., 2010, 2013, 2014; Lee et al., 2014; Salvatore et al., 2014). According to the current model, high expression of the inactivating enzyme D3 ensures strongly reduced intracellular TH levels in SCs in order to keep them in a proliferative state (Figure S3). Low intracellular TH concentrations seem to be a prerequisite for SC proliferation and survival. Indeed, Dentice et al. (2014) elegantly demonstrated that D3 acts a "survival factor" in these cells as inactivation of this enzyme specifically in SCs leads to caspase3-dependent apoptosis of activated stem cells. Absence of MCT8 and OATP1C1 in SCs possibly results in impaired TH uptake into these cells, thereby evoking low intracellular TH concentrations, which in turn keeps the SCs for a prolonged period in a proliferating state. Such a scenario would also explain the elevated number of PAX7-positive cells as well as the elevated D3 activities found in *M/O*-deficient muscle under resting conditions *in vivo* (Figure 6B).

Upon injury, SCs become activated, enter the cell cycle, and either divide symmetrically, thereby maintaining the pool of SCs, or asymmetrically to give rise to myogenic progenitor cells (Bentzinger et al., 2013a). Once activated, PAX7-positive SCs express the transcription factor MYOD, a master regulator of myogenesis that in turn regulates expression of downstream myogenic factors important for proper myogenesis (Bentzinger et al., 2012; von Maltzahn et al., 2012). Interestingly, upregulation of *MyoD* expression is controlled by local TH signaling via numerous pathways of which T3-stimulated *Foxo3* expression and, consecutively, *Foxo3*-induced *D2* expression represents one important mechanism (Dentice et al., 2010). Elevated D2 activities in turn locally generate "supraphysiological" T3 concentrations that are needed for robust induction of *MyoD* expression and thereby trigger the differentiation process (Figure S3). Indeed, inactivation of *D2* in mice has been shown to cause impaired differentiation of myoblasts similar to the phenotype described for *MyoD/Myf5*-deficient mice (Rudnicki et al., 1993). Thus, adequate and precise regulation of intracellular TH concentrations with low T3 levels in proliferating cells and a high-T3 condition in differentiating cells appears to be mandatory for proper myogenesis.

The strictly regulated TH action during myogenesis is obviously disturbed if *Mct8* and *Oatp1c1* are missing. Myofibers prepared from *M/O* DKO mice and cultured for 72 hr contained far fewer differentiated PAX7/MYOD double-positive and MYOD-positive cells, indicating that the differentiation process of PAX7-positive SCs is compromised (Figures 4C and 4D). Accordingly, an almost 50% reduction in Pax7/MYOD-positive cells was detected in muscles derived from *M/O* DKO mice when analyzed at 10 dpi. A significant drop in PAX7/MYOD cells after injury was even found in *M/O*-SC mice in which *Mct8* and *Oatp1c1* were exclusively deleted in *Pax7*-positive SCs (Figure 7C). Overall, these findings firmly demonstrate a critical cell-intrinsic role of MCT8 and OATP1C1 in SCs allowing proper timing of the differentiation process only in the presence of both transporters (Figure S3).

Are *Mct8/Oatp1c1*-deficient muscles able to fully regenerate in response to injury? Our *in vivo* studies indicate that the regeneration process is only transiently blocked if *Mct8* and *Oatp1c1* are absent. Myofiber size was temporarily reduced in TH transporter-deficient animals 5 and 10 dpi, but ultimately muscles fully regenerated to a normal size at 21 dpi with similar numbers of SCs (Figure 4). Possibly, elevated muscle T3 content together with the presence of other TH transporters such as MCT10 can partially compensate for a diminished cellular T3 transport caused by the absence of MCT8. In addition, and similarly to the situation in the brain (Bernal et al., 2015), the rise in muscle D2 activities in *Mct8*-deficient animals might provide another compensatory mechanism to counteract the compromised cellular T3 uptake. However, such a mechanism can only provide full compensation if sufficient amounts of T4 are available for local T3 production. Consequently, a combined deletion of *Mct8* and *Oatp1c1* that putatively compromises both T4 and T3 uptake into SCs affects proper SC differentiation to a much greater extent than inactivation of *Mct8* alone.

Overall, our data provide solid evidence for a unique gate-keeper function of MCT8 and OATP1C1 in SC activation and underscore the importance of a finely tuned TH signaling within the myogenic program. Unraveling the function of those TH transporters during regeneration of skeletal muscles might open additional therapeutic strategies for AHDS patients.

EXPERIMENTAL PROCEDURES

Animals

Mct8 KO mice were obtained from Deltagen and have been described previously (Trajkovic et al., 2007). *Oatp1c1* KO mice were generated from *Oatp1c1* fl/fl animals as reported before (Mayerl et al., 2012). Breeding pairs were set up as depicted previously in order to obtain WT, *Oatp1c1* KO, *Mct8* KO, and *Mct8*/*Oatp1c1* DKO mice on a C57BL/6 background (Mayerl et al., 2014). *Mct8* KO and *Oatp1c1* KO mice were genotyped as described previously (Mayerl et al., 2012; Trajkovic et al., 2007).

Conditional *Mct8* mutant mice (C57BL/6 background) were obtained from the KOMP repository (*Slc16a2*$^{tm1a(KOMP)Wtsi}$). Further information is provided in Supplemental Information.

Mct8 fl/fl mice were mated with *Oatp1c1* fl/fl mice and transgenic animals expressing a tamoxifen-inducible *Cre recombinase* driven by the *Pax7* promoter (Murphy et al., 2011). Detection of the *Pax7 CreERT2*/+ transgene was performed as stated elsewhere (Murphy et al., 2011). *Mct8* fl/fl, *Oatp1c1* fl/fl, *Pax7-CreERT2* mice were treated with tamoxifen to delete *Mct8* and *Oatp1c1* specifically in SCs (*M/O*-SC KO) as described previously (von Maltzahn et al., 2013). *Mct8* fl/fl, *Oatp1c1* fl/fl mice negative for the *CreERT2* transgene and treated with tamoxifen served as controls. Genomic DNA obtained from tail biopsies, brain, and gastrocnemius muscle were subjected to PCR.

Mice were kept at constant temperature (22°C) on a 12 hr light, 12 hr dark cycle and were provided with standard laboratory chow and water *ad libitum*. Animals were sacrificed by cervical dislocation at 2–4 months of age. Serum TH values were measured by radioimmunoassay as published elsewhere (Friedrichsen et al., 2003). For determination of muscle TH content and qPCR analysis, TA muscles were rapidly frozen in liquid nitrogen. Muscle T4 and T3 content was measured following rough homogenization and extraction of the tissues as described in detail by Reyns et al. (2002). Muscle tissues used for deiodinase activity assays were processed as described before (Friedrichsen et al., 2003).

For regeneration experiments, TA muscles of female mice at the age of 2.5–4 months were injured by intramuscular injection of 50 μL of CTX (10 μM in 0.9% NaCl) under isoflurane anesthesia and isolated 5, 10, or 21 dpi. Muscles were cross sectioned (12 μm) after embedding in cryoprotective medium (with 30% sucrose), and frozen in liquid nitrogen.

Affimetrix Microarray Data Acquisition

For cell-specific TH transporter expression analysis, we took advantage of microarray data that have been published by Price et al. (2014). In this study, quiescent SCs were isolated from heterozygous *Pax7-zsgreen* mice after a 30 min collagenase/dispase digestion and sorted for zsgreen expression (Price et al., 2014). The *Pax7-zsgreen* mice express the *zsgreen* reporter under control of the endogenous *Pax7* promoter. In addition, Price et al. (2014) sorted SCs from adult mice using alpha7 integrin in order to obtain activated SCs that were consecutively cultured under proliferating conditions (F10 medium with 20% FBS [Gibco] and 2.5 ng/mL fibroblast growth factor [Gibco]) for obtaining myoblasts, or under differentiating conditions (DMEM with 5% horse serum [HS; Gibco]) in order obtain myocytes (after 2 days in culture) and myotubes (after 5 days in culture), respectively. Unfortunately, activated SCs were not analyzed in this study.

Tissue Cultures

Single EDL myofibers were obtained from 2.5- to 4-month-old mice and cultured for 0 hr, 42 hr, or 72 hr (Bentzinger et al., 2013b). In brief, the EDL muscle was carefully removed, only handling the tendons, and digested with 2.5 mL of collagenase I (Sigma; final concentration, 0.2%) in DMEM for 45 min at 37°C under constant agitation. The muscle was then triturated using Pasteur pipettes coated with HS until single fibers came off. Single myofibers were transferred into culture medium (20% FBS in DMEM, 1% chicken embryo extract [Seralab]) in a 24-well plate coated with HS.

For inhibiting MCT8, Silychristin (25 μM, Sigma) was applied to the culture medium of WT and *Oatp1c1* KO-derived fiber cultures, whereas control fibers received equal amounts of the solvent (DMSO).

Immunofluorescence Studies

EDL myofibers were fixed with 2% paraformaldehyde (PFA) for 10 min, treated with 0.1 M glycine in PBS for 10 min, blocked, and permeabilized with PBS containing 10% HS and 0.2% Triton X-100. Subsequently, fibers were incubated with primary antibodies in PBS overnight at 4°C. Following washing with 0.2% Tween in PBS, fibers were incubated with fluorescence-labeled secondary antibodies raised in goat (1:1,000, Alexa Fluor 488 or 555; Invitrogen) and with Hoechst 33258 (1:10,000) to label cell nuclei. Thereafter, myofibers were washed, transferred on Superfrost slides, mounted with Paramount, and analyzed using an Olympus AX70 microscope.

Muscle cryosections (12 μm) were fixed with 2% PFA for 10 min, permeabilized with 0.1% Triton X-100/0.1 M glycine, blocked with MOM reagent (1:40 in PBS, Vector laboratories), and incubated with the respective primary antibody in PBS/5% goat serum overnight at 4°C. Subsequently, sections were incubated with fluorescently Alexa Fluor 488- or 555-labeled secondary antibodies (1:1,000) and Hoechst 33258 (1:10,000).

The following antibodies were used: rabbit anti-KI67 (1:500; Sigma-Aldrich), rabbit anti-LAMININ (1:1,000; L9393, Sigma-Aldrich), rabbit anti-MCT8 (1:500; HPA003353, Sigma-Aldrich), mouse anti-fast MHC (1:500; M4276, Sigma-Aldrich), mouse anti-slow MHC (1:500; M8421, Sigma-Aldrich), rabbit anti-MYOD (1:250; sc-304, Santa Cruz Biotechnology), rabbit anti-OATP1C1 (1:100; Mayerl et al., 2012), and mouse anti-PAX7 (undiluted; Developmental Studies Hybridoma Bank). TUNEL staining was performed using the *In Situ* Cell Death Detection Kit (catalog no. 11684817910, Roche) following the manufacturer's instructions.

qPCR

Detailed information on qPCR studies is provided in Supplemental Information.

Quantification

In EDL fiber cultures, numbers of total MYOD-positive, MYOD-only-positive, total PAX7-positive, PAX7-only-positive, and PAX7/MYOD double-positive cells were counted per cell cluster

72 hr after fiber isolation. Myofiber numbers of whole plantaris and soleus cross-sections were determined by staining 3–6 consecutive sections for LAMININ and the respective MHC antibodies. TA muscle fiber diameter was assessed by measuring the minimal fiber feret (defined as the minimum distance of parallel tangents at opposing borders of the myofiber). For that purpose, whole cross-sections of LAMININ stained muscles were analyzed with an AxioObserver (Zeiss) utilizing the mosaic function provided by the Zen software (Zeiss) to automatically stitch the images. Quantification of fiber types was conducted manually by counting the number of slow and fast MHC-positive fibers and dividing them by the number of total fibers in order to get the percentages of slow and fast MHC-positive fibers per muscle respectively. Following CTX injury, only those muscle fibers were included in the analysis that displayed centrally located nuclei. Numbers of MYOD-positive, PAX7-positive, and PAX7/MYOD double-positive cells were counted per area.

Tamoxifen treatment efficiency was calculated by counting the number of PAX7-positive cell clusters either showing or lacking TH transporter immunofluorescent signals along 10 *M/O*-SC KO EDL-derived myofibers 72 hr after isolation.

To quantify cell culture results, six to eight independent images per sample and condition have been investigated. For proper comparison between different samples and conditions, only cross-sections of the muscle's mid-belly regions were used in these analyses, immunostainings were always performed in parallel, images were acquired with the same settings, and all measurements were performed in a blinded manner.

Statistics

Values represent mean + SEM from at least three animals per genotype and time point. For multigroup comparisons, two-way ANOVA was performed (2 × 2 factorial ANOVA; factor A, WT versus *Oatp1c1* KO; factor B, WT versus *Mct8* KO) using Daniels XL Toolbox add-in for Microsoft Excel followed by Bonferroni-Holm post hoc testing. Statistical significance between control and *M/O*-SC KO mice was assessed by unpaired Student's t test (Microsoft Excel). A p value less than 0.05 was considered significant.

Study Approval

All animal procedures were in accordance with the European Union (EU) directive 2010/63/EU and approved by the Animal Welfare Committee of the Thüringer Landesamt für Lebensmittelsicherheit und Verbraucherschutz (03-011/14 and 03-48/16; TLV; Bad Langensalza, Germany) and the Landesamt für Natur, Umwelt und Verbraucherschutz Nordrhein-Westfalen (84-02-04.2017.A219; LANUV; Recklinghausen, Germany), respectively.

SUPPLEMENTAL INFORMATION

Supplemental Information includes Supplemental Experimental Procedures and three figures and can be found with this article online at https://doi.org/10.1016/j.stemcr.2018.03.021.

AUTHOR CONTRIBUTIONS

S.M., J.v.M., and H.H. designed experiments, analyzed data, interpreted results, and wrote the manuscript. S.M., M.S., D.D., S.S.H., and J.v.M. performed *in vivo* and *in vitro* experiments on myogenesis and muscle regeneration. C.K. provided valuable reagents and advice on microscopy. A.B., V.M.D., S.L., and T.J.V. determined TH levels, tissue TH content, and deiodinase activities. M.S. and D.D. contributed equally, and H.H. and J.v.M. contributed equally.

ACKNOWLEDGMENTS

This work was supported by grants from the DFG to J.v.M. (MA-3975/2-1) and H.H. (HE3418/7-1; HE3418/8-1 within the SPP1629). We would like to thank Stefanie Rosenhain (FLI Jena), Selmar Leeuwenburgh (EMC Rotterdam), and Lut Noterdaeme (KU Leuven) for excellent technical assistance. We are grateful to D. Salvatore and M. Dentice for helpful discussions.

Received: November 9, 2017
Revised: March 27, 2018
Accepted: March 28, 2018
Published: April 26, 2018

REFERENCES

Ambrosio, R., De Stefano, M.A., Di Girolamo, D., and Salvatore, D. (2017). Thyroid hormone signaling and deiodinase actions in muscle stem/progenitor cells. Mol. Cell Endocrinol. *459*, 79–83.

Bentzinger, C.F., Wang, Y.X., Dumont, N.A., and Rudnicki, M.A. (2013a). Cellular dynamics in the muscle satellite cell niche. EMBO Rep. *14*, 1062–1072.

Bentzinger, C.F., Wang, Y.X., and Rudnicki, M.A. (2012). Building muscle: molecular regulation of myogenesis. Cold Spring Harb. Perspect. Biol. *4*. https://doi.org/10.1101/cshperspect.a008342.

Bentzinger, C.F., Wang, Y.X., von Maltzahn, J., Soleimani, V.D., Yin, H., and Rudnicki, M.A. (2013b). Fibronectin regulates Wnt7a signaling and satellite cell expansion. Cell Stem Cell *12*, 75–87.

Bernal, J., Guadaño-Ferraz, A., and Morte, B. (2015). Thyroid hormone transporters–functions and clinical implications. Nat. Rev. Endocrinol. *11*, 506.

Bianco, A.C., Salvatore, D., Gereben, B., Berry, M.J., and Larsen, P.R. (2002). Biochemistry, cellular and molecular biology, and physiological roles of the iodothyronine selenodeiodinases. Endocr. Rev. *23*, 38–89.

Ceballos, A., Belinchon, M.M., Sanchez-Mendoza, E., Grijota-Martinez, C., Dumitrescu, A.M., Refetoff, S., Morte, B., and Bernal, J. (2009). Importance of monocarboxylate transporter 8 for the blood-brain barrier-dependent availability of 3,5,3′-triiodo-L-thyronine. Endocrinology *150*, 2491–2496.

Chang, N.C., Chevalier, F.P., and Rudnicki, M.A. (2016). Satellite cells in muscular dystrophy - lost in polarity. Trends Mol. Med. *22*, 479–496.

Dentice, M., Ambrosio, R., Damiano, V., Sibilio, A., Luongo, C., Guardiola, O., Yennek, S., Zordan, P., Minchiotti, G., Colao, A., et al. (2014). Intracellular inactivation of thyroid hormone is a survival mechanism for muscle stem cell proliferation and lineage progression. Cell Metab. *20*, 1038–1048.

Dentice, M., Marsili, A., Ambrosio, R., Guardiola, O., Sibilio, A., Paik, J.H., Minchiotti, G., DePinho, R.A., Fenzi, G., Larsen, P.R.,

et al. (2010). The FoxO3/type 2 deiodinase pathway is required for normal mouse myogenesis and muscle regeneration. J. Clin. Invest. *120*, 4021–4030.

Dentice, M., Marsili, A., Zavacki, A., Larsen, P.R., and Salvatore, D. (2013). The deiodinases and the control of intracellular thyroid hormone signaling during cellular differentiation. Biochim. Biophys. Acta *1830*, 3937–3945.

Di Cosmo, C., Liao, X.H., Ye, H., Ferrara, A.M., Weiss, R.E., Refetoff, S., and Dumitrescu, A.M. (2013). Mct8-deficient mice have increased energy expenditure and reduced fat mass that is abrogated by normalization of serum T3 levels. Endocrinology *154*, 4885–4895.

Dumitrescu, A.M., Liao, X.H., Best, T.B., Brockmann, K., and Refetoff, S. (2004). A novel syndrome combining thyroid and neurological abnormalities is associated with mutations in a monocarboxylate transporter gene. Am. J. Hum. Genet. *74*, 168–175.

Dumitrescu, A.M., Liao, X.H., Weiss, R.E., Millen, K., and Refetoff, S. (2006). Tissue-specific thyroid hormone deprivation and excess in monocarboxylate transporter (mct) 8-deficient mice. Endocrinology *147*, 4036–4043.

Friedrichsen, S., Christ, S., Heuer, H., Schäfer, M.K., Mansouri, A., Bauer, K., and Visser, T.J. (2003). Regulation of iodothyronine deiodinases in the Pax8-/- mouse model of congenital hypothyroidism. Endocrinology *144*, 777–784.

Friesema, E.C., Ganguly, S., Abdalla, A., Manning Fox, J.E., Halestrap, A.P., and Visser, T.J. (2003). Identification of monocarboxylate transporter 8 as a specific thyroid hormone transporter. J. Biol. Chem. *278*, 40128–40135.

Friesema, E.C., Grueters, A., Biebermann, H., Krude, H., von Moers, A., Reeser, M., Barrett, T.G., Mancilla, E.E., Svensson, J., Kester, M.H., et al. (2004). Association between mutations in a thyroid hormone transporter and severe X-linked psychomotor retardation. Lancet *364*, 1435–1437.

Friesema, E.C., Jansen, J., Jachtenberg, J.W., Visser, W.E., Kester, M.H., and Visser, T.J. (2008). Effective cellular uptake and efflux of thyroid hormone by human monocarboxylate transporter 10. Mol. Endocrinol. *22*, 1357–1369.

Friesema, E.C., Jansen, J., Milici, C., and Visser, T.J. (2005). Thyroid hormone transporters. Vitam. Horm. *70*, 137–167.

Herzovich, V., Vaiani, E., Marino, R., Dratler, G., Lazzati, J.M., Tilitzky, S., Ramirez, P., Iorcansky, S., Rivarola, M.A., and Belgorosky, A. (2007). Unexpected peripheral markers of thyroid function in a patient with a novel mutation of the MCT8 thyroid hormone transporter gene. Horm. Res. *67*, 1–6.

Heuer, H., and Visser, T.J. (2009). Minireview: pathophysiological importance of thyroid hormone transporters. Endocrinology *150*, 1078–1083.

Heuer, H., and Visser, T.J. (2013). The pathophysiological consequences of thyroid hormone transporter deficiencies: insights from mouse models. Biochim. Biophys. Acta *1830*, 3974–3978.

Ito, K., Uchida, Y., Ohtsuki, S., Aizawa, S., Kawakami, H., Katsukura, Y., Kamiie, J., and Terasaki, T. (2011). Quantitative membrane protein expression at the blood-brain barrier of adult and younger cynomolgus monkeys. J. Pharm. Sci. *100*, 3939–3950.

Johannes, J., Jayarama-Naidu, R., Meyer, F., Wirth, E.K., Schweizer, U., Schomburg, L., Köhrle, J., and Renko, K. (2016). Silychristin, a flavonolignan derived from the milk thistle, is a potent inhibitor of the thyroid hormone transporter MCT8. Endocrinology *157*, 1694–1701.

Lee, J.W., Kim, N.H., and Milanesi, A. (2014). Thyroid hormone signaling in muscle development, repair and metabolism. J. Endocrinol. Diabetes Obes. *2*, 1046.

Lepper, C., Partridge, T.A., and Fan, C.M. (2011). An absolute requirement for Pax7-positive satellite cells in acute injury-induced skeletal muscle regeneration. Development *138*, 3639–3646.

Mayerl, S., Muller, J., Bauer, R., Richert, S., Kassmann, C.M., Darras, V.M., Buder, K., Boelen, A., Visser, T.J., and Heuer, H. (2014). Transporters MCT8 and OATP1C1 maintain murine brain thyroid hormone homeostasis. J. Clin. Invest. *124*, 1987–1999.

Mayerl, S., Visser, T.J., Darras, V.M., Horn, S., and Heuer, H. (2012). Impact of Oatp1c1 deficiency on thyroid hormone metabolism and action in the mouse brain. Endocrinology *153*, 1528–1537.

Milanesi, A., Lee, J.W., Kim, N.H., Liu, Y.Y., Yang, A., Sedrakyan, S., Kahng, A., Cervantes, V., Tripuraneni, N., Cheng, S.Y., et al. (2016). Thyroid hormone receptor α plays an essential role in male skeletal muscle myoblast proliferation, differentiation, and response to injury. Endocrinology *157*, 4–15.

Milanesi, A., Lee, J.W., Yang, A., Liu, Y.Y., Sedrakyan, S., Cheng, S.Y., Perin, L., and Brent, G.A. (2017). Thyroid hormone receptor α is essential to maintain the satellite cell niche during skeletal muscle injury and sarcopenia of aging. Thyroid *10*, 1316–1322.

Murphy, M.M., Lawson, J.A., Mathew, S.J., Hutcheson, D.A., and Kardon, G. (2011). Satellite cells, connective tissue fibroblasts and their interactions are crucial for muscle regeneration. Development *138*, 3625–3637.

Müller, J., Mayerl, S., Visser, T.J., Darras, V.M., Boelen, A., Frappart, L., Mariotta, L., Verrey, F., and Heuer, H. (2014). Tissue-specific alterations in thyroid hormone homeostasis in combined Mct10 and Mct8 deficiency. Endocrinology *155*, 315–325.

Price, F.D., von Maltzahn, J., Bentzinger, C.F., Dumont, N.A., Yin, H., Chang, N.C., Wilson, D.H., Frenette, J., and Rudnicki, M.A. (2014). Inhibition of JAK-STAT signaling stimulates adult satellite cell function. Nat. Med. *20*, 1174–1181.

Reyns, G.E., Janssens, K.A., Buyse, J., Kuhn, E.R., and Darras, V.M. (2002). Changes in thyroid hormone levels in chicken liver during fasting and refeeding. Comp. Biochem. Physiol. B Biochem. Mol. Biol. *132*, 239–245.

Roberts, L.M., Woodford, K., Zhou, M., Black, D.S., Haggerty, J.E., Tate, E.H., Grindstaff, K.K., Mengesha, W., Raman, C., and Zerangue, N. (2008). Expression of the thyroid hormone transporters monocarboxylate transporter-8 (SLC16A2) and organic ion transporter-14 (SLCO1C1) at the blood-brain barrier. Endocrinology *149*, 6251–6261.

Rudnicki, M.A., Schnegelsberg, P.N., Stead, R.H., Braun, T., Arnold, H.H., and Jaenisch, R. (1993). MyoD or Myf-5 is required for the formation of skeletal muscle. Cell *75*, 1351–1359.

Salvatore, D., Simonides, W.S., Dentice, M., Zavacki, A.M., and Larsen, P.R. (2014). Thyroid hormones and skeletal muscle–new

insights and potential implications. Nat. Rev. Endocrinol. *10*, 206–214.

Schwartz, C.E., May, M.M., Carpenter, N.J., Rogers, R.C., Martin, J., Bialer, M.G., Ward, J., Sanabria, J., Marsa, S., Lewis, J.A., et al. (2005). Allan-Herndon-Dudley syndrome and the monocarboxylate transporter 8 (MCT8) gene. Am. J. Hum. Genet. *77*, 41–53.

Soukup, T., and Smerdu, V. (2015). Effect of altered innervation and thyroid hormones on myosin heavy chain expression and fiber type transitions: a mini-review. Histochem. Cell Biol. *143*, 123–130.

Trajkovic, M., Visser, T.J., Mittag, J., Horn, S., Lukas, J., Darras, V.M., Raivich, G., Bauer, K., and Heuer, H. (2007). Abnormal thyroid hormone metabolism in mice lacking the monocarboxylate transporter 8. J. Clin. Invest. *117*, 627–635.

Visser, W.E., Friesema, E.C., and Visser, T.J. (2011). Minireview: thyroid hormone transporters: the knowns and the unknowns. Mol. Endocrinol. *25*, 1–14.

von Maltzahn, J., Chang, N.C., Bentzinger, C.F., and Rudnicki, M.A. (2012). Wnt signaling in myogenesis. Trends Cell Biol. *22*, 602–609.

von Maltzahn, J., Jones, A.E., Parks, R.J., and Rudnicki, M.A. (2013). Pax7 is critical for the normal function of satellite cells in adult skeletal muscle. Proc. Natl. Acad. Sci. USA *110*, 16474–16479.

Wirth, E.K., Roth, S., Blechschmidt, C., Holter, S.M., Becker, L., Racz, I., Zimmer, A., Klopstock, T., Gailus-Durner, V., Fuchs, H., et al. (2009). Neuronal 3′,3,5-triiodothyronine (T3) uptake and behavioral phenotype of mice deficient in Mct8, the neuronal T3 transporter mutated in Allan-Herndon-Dudley syndrome. J. Neurosci. *29*, 9439–9449.

Stem Cell Reports, Volume *10*

Supplemental Information

Thyroid Hormone Transporters MCT8 and OATP1C1 Control Skeletal Muscle Regeneration

Steffen Mayerl, Manuel Schmidt, Denica Doycheva, Veerle M. Darras, Sören S. Hüttner, Anita Boelen, Theo J. Visser, Christoph Kaether, Heike Heuer, and Julia von Maltzahn

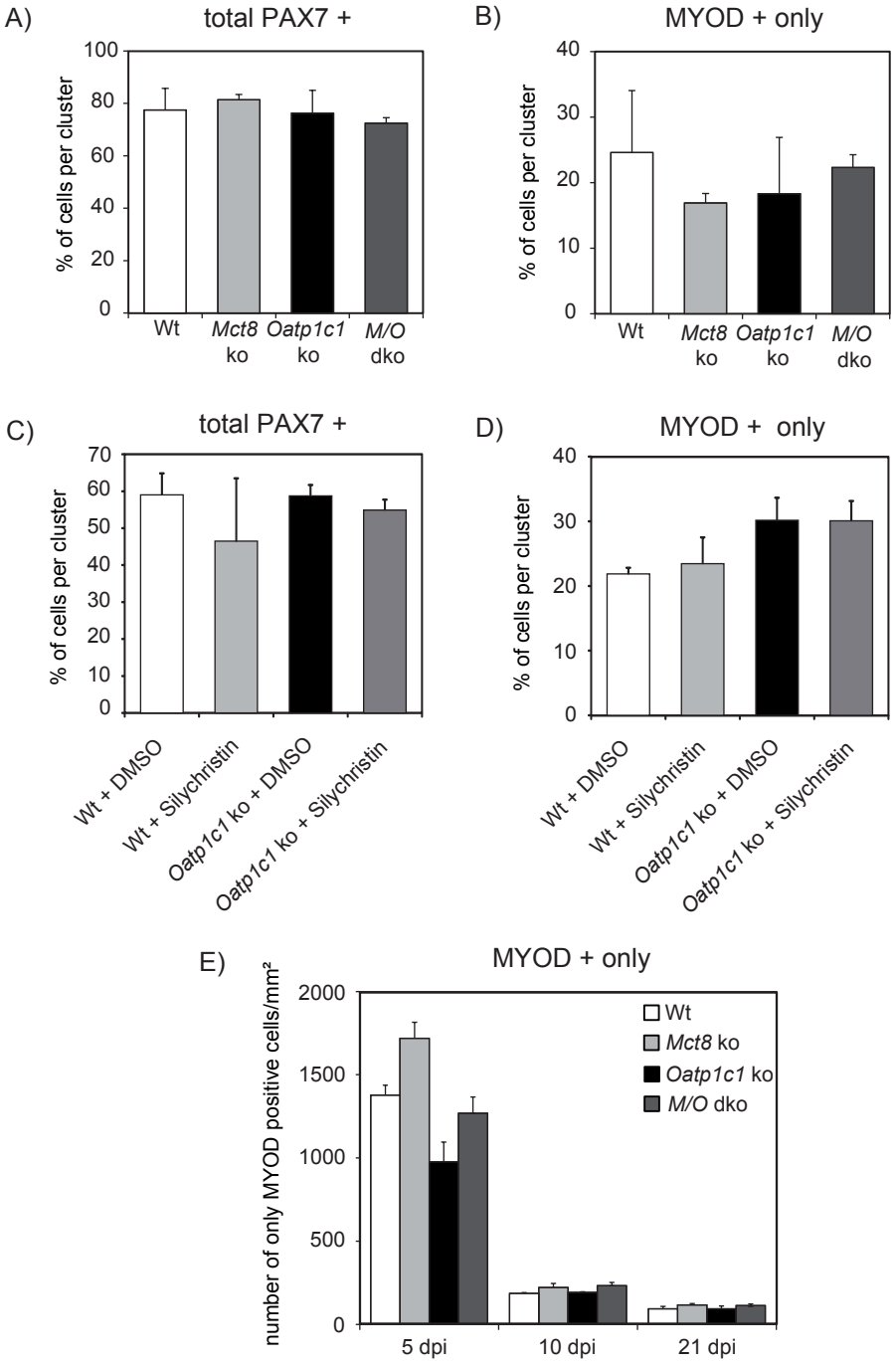
A)
total PAX7 +
% of cells per cluster
100
80
60
40
20
0
Wt
Mct8 ko
Oatp1c1 ko
M/O dko
B)
MYOD + only
% of cells per cluster
40
30
20
10
0
Wt
Mct8 ko
Oatp1c1 ko
M/O dko
C)
total PAX7 +
% of cells per cluster
70
60
50
40
30
20
10
0
Wt + DMSO
Wt + Silychristin
Oatp1c1 ko + DMSO
Oatp1c1 ko + Silychristin
D)
MYOD + only
% of cells per cluster
40
30
20
10
0
Wt + DMSO
Wt + Silychristin
Oatp1c1 ko + DMSO
Oatp1c1 ko + Silychristin
E)
MYOD + only
number of only MYOD positive cells/mm²
2000
1500
1000
500
0
Wt
Mct8 ko
Oatp1c1 ko
M/O dko
5 dpi
10 dpi
21 dpi

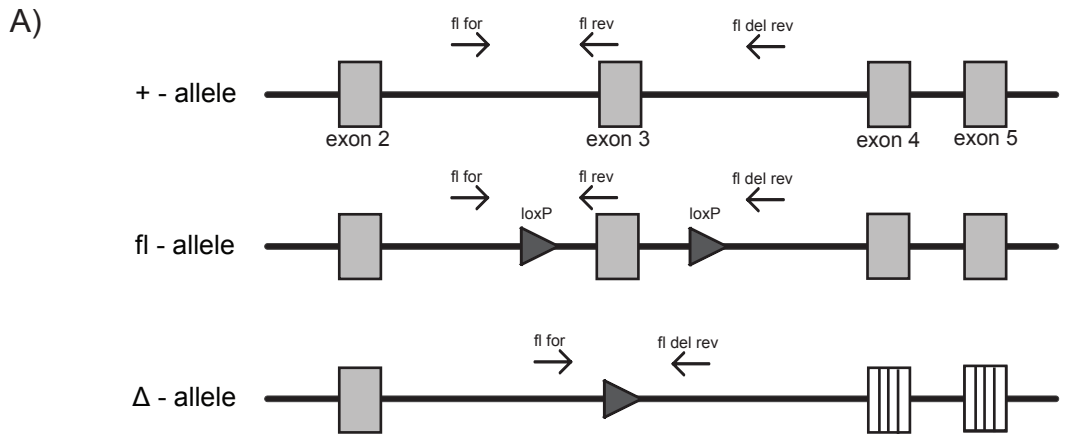
A)
fl for
fl rev
fl del rev
+ - allele
exon 2
exon 3
exon 4
exon 5
fl for
fl rev
fl del rev
loxP
loxP
fl - allele
fl for
fl del rev
Δ - allele

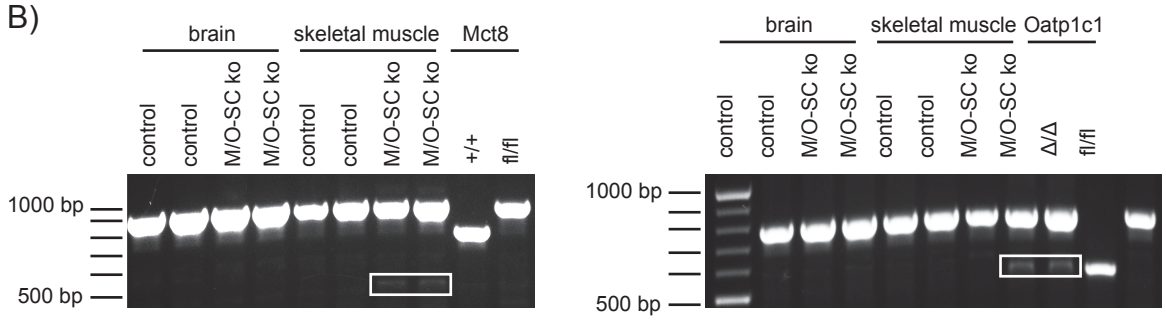
B)
brain
skeletal muscle
Mct8
control
control
M/O-SC ko
M/O-SC ko
control
control
M/O-SC ko
M/O-SC ko
+/+
fl/fl
1000 bp
500 bp
brain
skeletal muscle
Oatp1c1
control
control
M/O-SC ko
M/O-SC ko
control
control
M/O-SC ko
M/O-SC ko
Δ/Δ
fl/fl
1000 bp
500 bp

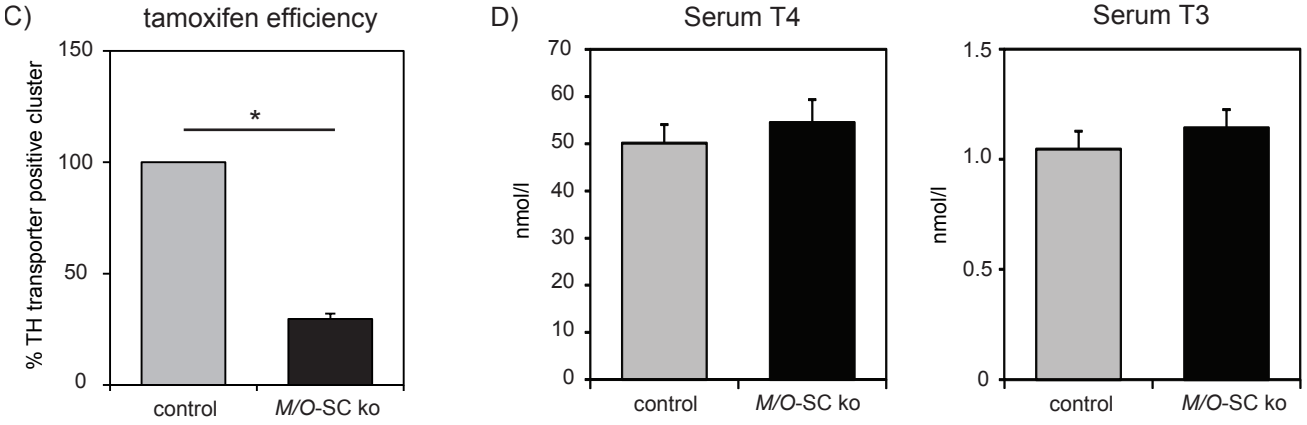
C)
tamoxifen efficiency
% TH transporter positive cluster
150
100
50
0
*
control
M/O-SC ko
D)
Serum T4
nmol/l
70
60
50
40
30
20
10
0
control
M/O-SC ko
Serum T3
nmol/l
1.5
1.0
0.5
0
control
M/O-SC ko

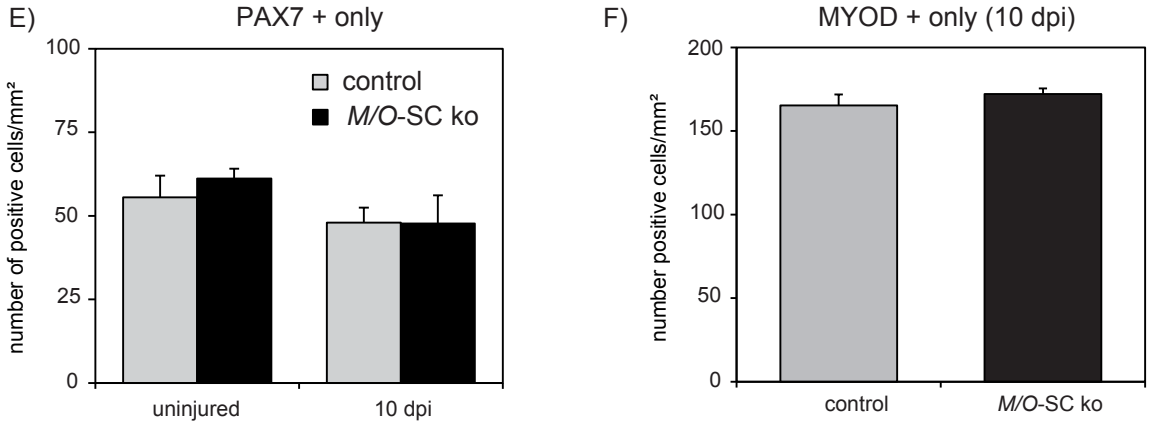
E)
PAX7 + only
number of positive cells/mm²
100
75
50
25
0
control
M/O-SC ko
uninjured
10 dpi
F)
MYOD + only (10 dpi)
number positive cells/mm²
200
150
100
50
0
control
M/O-SC ko

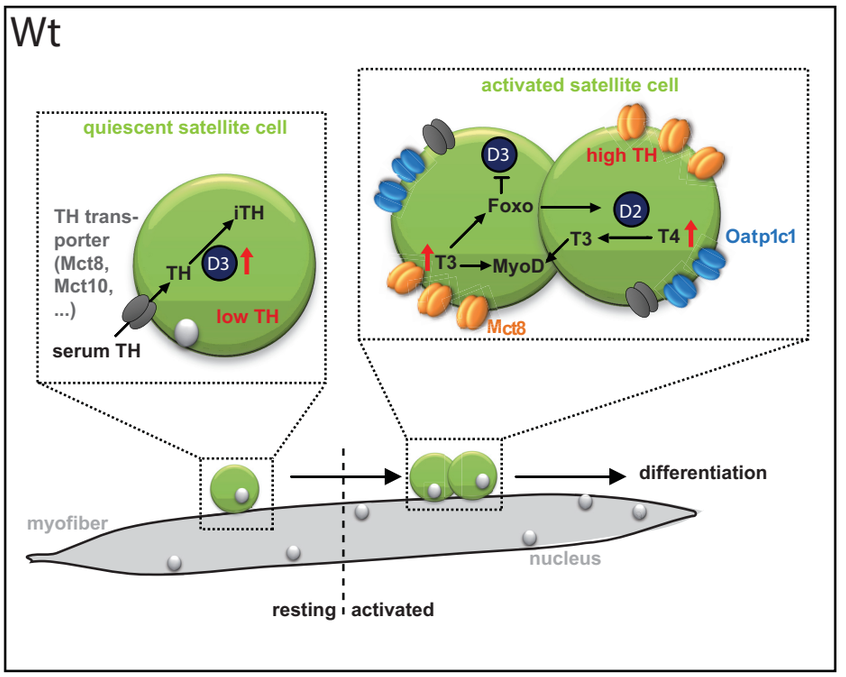
Wt
activated satellite cell
quiescent satellite cell
D3
high TH
Foxo
D2
T3
T4
Oatp1c1
T3
MyoD
Mct8
TH trans-
porter
(Mct8,
Mct10,
...)
iTH
TH
D3
low TH
serum TH
differentiation
myofiber
nucleus
resting
activated

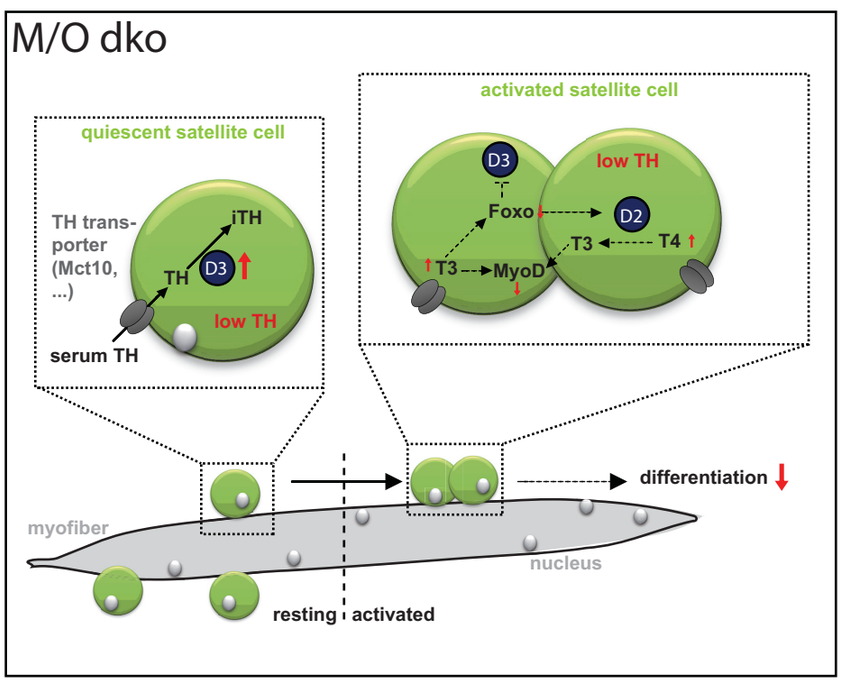
M/O dko
activated satellite cell
quiescent satellite cell
D3
low TH
Foxo
D2
T3
T4
T3
MyoD
TH trans-
porter
(Mct10,
...)
iTH
TH
D3
low TH
serum TH
differentiation
myofiber
nucleus
resting
activated

Suppl. Fig.1: Muscle stem cell activation *in vitro* and *in vivo.*

Wt, *Mct8* and/or *Oatp1c1* deficient primary EDL myofibers (n=3) were cultured for 72 h, incubated with antibodies directed against PAX7 and the activation and differentiation marker MYOD, and marker positive cells were quantified. No differences in the percentage of PAX7 positive nuclei (A) nor in the percentage of only MYOD positive myoblasts per cluster (B) were observed in TH transporter ko mice. Similarly, incubation of Wt (n=4) and *Oatp1c1* ko (n=6) EDL fibers with DMSO alone or Silychristin (25 µM) for 72 h followed by staining for PAX7 and MYOD did not generate effects on the overall percentage of PAX7 positive nuclei per cluster (C) nor the abundance of only MYOD positive myoblasts (D). (E) 5, 10, and 21 days after CTX injury the number of only MYOD immunopositive myoblasts was quantified in Wt, *Mct8* ko, *Oatp1c1* ko, and *M/O* dko animals, but did not reveal significant alterations between the genotypes. Group mean+SEM are shown. n = 4 Wt 5 dpi, *M/O* dko 5 dpi; n=3 all other groups. 2-way ANOVA and Bonferroni-Holm post hoc testing.

Suppl. Fig.2: Generation and analysis of SC-specific *M/O* deficient (*M/O*-SC ko) mice.

(A) Schematic illustration of the targeting strategy to generate conditional Mct8 mutant mice by flanking exon 3 of the murine *Mct8* gene by loxP sites (fl-allele; dark grey arrowheads). Cre-mediated excision of exon 3 results in a frameshift mutation from exon 4 to 5 (Δ-allele; Δ-allele dashed boxes). Black arrows indicate binding sites for genotyping primers. (B) Genotyping PCRs were conducted on brain and skeletal muscle (gastrocnemius) biopsies for *Mct8* (left panel) and *Oatp1c1* (right panel). In brain samples of tamoxifen-induced control and *M/O*-SC ko mice, only PCR products specific for the respective *Mct8* and *Oatp1c1* fl-allele could be detected. Likewise, PCR products depicting the respective *Mct8* and *Oatp1c1* delta allele were absent

from control skeletal muscle samples but could be detected in skeletal muscle of *M/O*-SC ko mice (white boxes). Tail biopsies of *Mct8* +/+ and *Mct8* fl/fl mice as well as *Oatp1c1* Δ/Δ and fl/fl animals served as controls. (C) EDL cultures prepared from control and *M/O*-SC ko mice (n=3) were immunostained for PAX7, MCT8 and OATP1C1 72 h after isolation. Only 29.7% of all clusters contained PAX7 positive cells that were also immunopositive for either MCT8 or OATP1C1 indicating that tamoxifen treatment was efficient in activating both TH transporters in about 70% of all satellite cells. (D) Circulating T4 and T3 concentrations do not differ between tamoxifen-treated control and *M/O*-SC ko animals (n=9). (E) PAX7 and MYOD immunopositive cells were counted in cryosections of CTX injured TA muscle 10 dpi and the respective contralateral uninjured muscles. Quantification of PAX7 positive only satellite cells (E) and MYOD only positive myoblasts (F) revealed no differences (n=4). Group mean+SEM are shown. * $p < 0.05$. unpaired 2-tailed Student's *t* test.

Suppl. Fig.3: Model of TH transporter-dependent activation of SCs.

SCs (green) located adjacent to mature muscle fibers (grey) express basal amounts of TH transporters such as MCT8 or MCT10 (in dark grey) in order to sense circulating T3 and T4 concentrations in the resting state. In quiescent SCs, T3 and T4 are inactivated (iTH) and TH levels are kept low by D3 activity. Following activation of muscle stem cells due to various stimuli (e.g. injury), MCT8 (orange) levels rise while OATP1C1 (blue) becomes transiently expressed thereby consequently accelerating uptake of T3 and T4 into activated SCs. In a T3-induced feed-forward loop FOXO transcription factors inhibit D3 action while D2 is induced in turn generating supraphysiological T3 concentrations in activated SCs (Dentice et al., 2010). Increased cellular TH content is essential for timely differentiation and progression within the myogenic program by inducing expression of the master regulator of myogenesis, *MyoD*. In *M/O* dko mice, SC might still sense circulating TH via MCT10. However, upon activation, major TH uptake routes are blocked most

likely decreasing the efficiency of the feed-forward loop thereby delaying differentiation programs and hence muscle regeneration.

Supplementary experimental procedures:

qPCR

Total tissue RNA was isolated using the NucleoSpin® RNA II Kit (Macherey-Nagel). Synthesis of cDNA was performed using the Transcriptor High Fidelity cDNA Synthesis Kit (Roche). To exclude the presence of genomic DNA, one sample without reverse transcriptase was included as well. Quantitative Real-Time PCR (qPCR) was performed using the iQ SYBR Green Supermix (Bio-Rad) and the CFX Connect™ Real-Time PCR Detection System (Bio-Rad). Ten nanograms of cDNA were employed in one qPCR reaction. Three to five samples per genotype were subjected to the analysis in triplicate. As a housekeeping gene for normalization *Glyceraldehyde 3-phosphate dehydrogenase* (*Gapdh*) was used. The following primers were chosen to generate the PCR fragments: *Gapdh* 5'-ATGCCAGTGAGCTTCCCGTC-3' and 5'-CATCACCATCTTCCAGGAGC-3'; Hr 5'-AAGCTAAATAGGGGATCCTG-3' and 5'- ATTTGTAGAACGGACCACAC-3'; MHCI 5'-AGTCCCAGGTCAACAAGCTG-3' and 5'-TTCCACCTAAAGGGCTGTTG-3'; *MhcIIa* 5'-AGTCCCAGGTCAACAAGCTG-3' and 5'-GCATGACCAAAGGTTTCACA-3'; *MhcIIb* 5'-AGTCCCAGGTCAACAAGCTG-3' and 5'-TTTCTCCTGTCACCTCTCAACA-3'; *MhcIIx* 5'-AGTCCCAGGTCAACAAGCTG-3' and 5'-CCTCCTGTGCTTTCCTTCAG-3'; *MyoD* 5'-CTACAGTGGCGACTCAGAT-3' and 5'-CACTGTAGTAGGCGGTGTC-3';. The annealing temperature was 55°C for all primer pairs.